Electronic properties of hole- and electron-doped T'-, T^*-, and infinite-layer-type high-T_c cuprates

M. Klauda, J. Markl, C. Fink, P. Lunz, G. Saemann-Ischenko, F. Rau,*
K.-J. Range,* R. Seemann,† and R. L. Johnson†
Physikalisches Institut, Universität Erlangen-Nürnberg, Erwin-Rommel-Strasse 1, D-W 8520 Erlangen, Germany
(Received 23 November 1992)

We compare the electronic structure of *n*-type and *p*-type dopable high-T_c cuprates, namely the hole-doped $Nd_{1.4}Ce_{0.2}Sr_{0.4}CuO_{4-\delta}$ (T^*) system as well as the electron-doped $Nd_{2-x}Ce_xCuO_{4-\delta}$ (T') and $Sr_{0.85}Nd_{0.15}CuO_{2-\delta}$ ("infinite-layer") systems. Investigations were done mainly by means of core-level and valence-band photoemission spectroscopy. Also we performed auxiliary measurements of Hall effect and magnetic susceptibility. From the investigations on the Cu-O layers we propose that one criterion for electron dopability in high-T_c cuprates is a comparatively high value of the Cu 3*d* Coulomb interaction U_{dd}. This is concluded from model calculations on core-level and valence-band spectra. Also the superconducting infinite-layer compound $Sr_{0.85}Nd_{0.15}CuO_{2-\delta}$ exhibits (besides a remarkably low Cu-O hybridization) this enhanced value of U_{dd}. For the rare-earth layers of T' and T^* we find small but characteristic differences in the electronic properties (Nd-O-hybridization and charge-transfer energy), which can be attributed to structural differences. Crystal-field splitting of Nd 4*f* levels and antiferromagnetic coupling of Nd^{3+} moments in $Nd_{1.85}Ce_{0.15}CuO_{4-\delta}$ and $Nd_{1.4}Ce_{0.2}Sr_{0.4}CuO_{4-\delta}$ have been investigated by evaluation of the magnetic susceptibility. The dopant ions cerium for T' and T^* and neodymium for $Sr_{0.85}Nd_{0.15}CuO_{2-\delta}$ are found to be tetra- and trivalent, respectively, which confirms again that the infinite-layer compound is an electron-doped cuprate.

I. INTRODUCTION

Much experimental and theoretical work has been done on the question of what causes an oxocuprate to achieve metallic behavior and superconductivity either by electronlike or holelike doping. A few months before the discovery of *n*-type high-temperature superconductors (HTSC's),[1,2] namely, the $M_{2-x}Ce_xCuO_{4-\delta}$ systems of T' structure [M=Pr, Nd, Sm, and less later, Eu (Ref. 3)], superconductivity was found in the *p*-type conducting $Nd_{1.4}Ce_{0.2}Sr_{0.4}CuO_{4-\delta}$ compound by Akimitsu *et al.*[4] Both systems are well suited for comparative investigations on the origin of *n*- or *p*-type dopability due to their very close structural relationship (as will be described below) and due to similar constituents (Cu and Nd) in the characteristical structural elements. The recent discovery of supposed *n*-type high-temperature superconductivity in the $Sr_{1-x}Nd_xCuO_{2-\delta}$ systems by Smith *et al.*[5] offers a further possibility to characterize the essential structural and electronic features of electron-dopable HTSC's by comparison of the infinite-layer compound $Sr_{1-x}Nd_xCuO_{2-\delta}$ with the "old" $M_{2-x}Ce_xCuO_{4-\delta}$ systems.

As mentioned above, the first superconducting T^* system $Nd_{1.4}Ce_{0.2}Sr_{0.4}CuO_{4-\delta}$ was found in 1988.[4] Neutron-scattering structure refinements by Sawa *et al.*[6] and Izumi *et al.*[7] confirmed the T^* structure to be a hybrid of the well-known T'-(Nd_2CuO_4) (Refs. 8 and 9) and T-(La_2CuO_4)[10] systems, being composed of alternating slabs of T and T' parts. Therefore each copper ion has a pyramidal surrounding of five oxygen ions in contrast to the octahedral and planar O coordinations of Cu in T and T', respectively (see Fig. 1). All T^* compounds known so far are of the composition $(M_{1-x-y}M'_xSr_y)_2CuO_{4-\delta}$, M and M' being rare-earth ions such as La, Nd, Pr (for M) and Ce, Sm, Eu, or Gd (for M').[11–15] Formation of the single-phase T^* structure (instead of the competing,

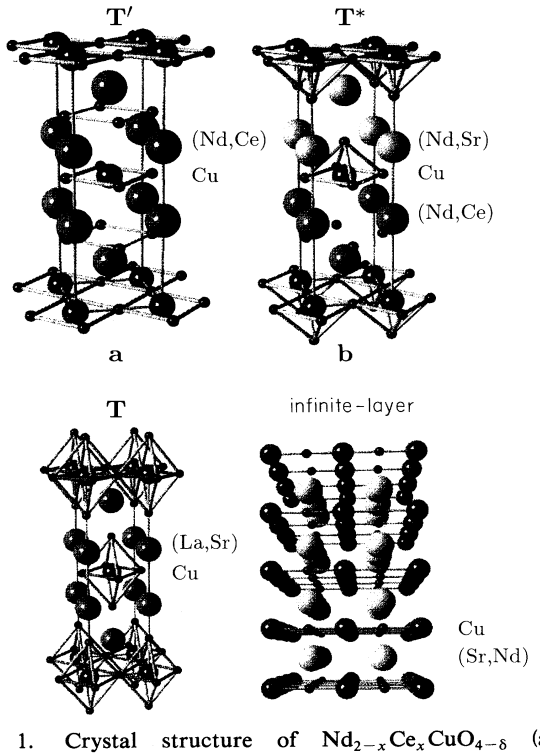

FIG. 1. Crystal structure of $Nd_{2-x}Ce_xCuO_{4-\delta}$ (a), $Nd_{1.4}Ce_{0.2}Sr_{0.4}CuO_{4-\delta}$ (b), and $La_{2-x}Sr_xCuO_{4-\delta}$ (c), as well as $Sr_{1-x}Nd_xCuO_{2-\delta}$ (d).

0163-1829/93/48(2)/1217(16)/$06.00 ©1993 The American Physical Society

more stable T and T' structures) strongly depends on the mean size of the rare-earth element (M,M') and on the amount of Sr doping.[16–18]

A common feature of all T^* systems obviously is a positive sign of charge carriers.[15,19,20] Especially for $Nd_{1.4}Ce_{0.2}Sr_{0.4}CuO_{4-\delta}$ the temperature dependence of the Hall coefficient $|R_H(T)|$—aside from the sign—is quite similar to the n-doped pendant $Nd_{1.85}Ce_{0.15}CuO_{4-\delta}$.[2,21] For superconducting compounds among the T^*-family transition temperatures range from below 2 K ($La_{0.9}Gd_{0.9}Sr_{0.2}CuO_{4-\delta}$) up to 30 K for high-pressure-prepared $Nd_{1.4}Ce_{0.2}Sr_{0.4}CuO_{4-\delta}$.[22]

For our investigations we chose the $Nd_{1.4}Ce_{0.2}Sr_{0.4}CuO_{4-\delta}$ compound since *both* structure *and* constituents are very similar to the n-type $Nd_{2-x}Ce_xCuO_{4-\delta}$ compounds. Furthermore, the T^* system at the utmost borderline to electron-doped[23–27] high-temperature superconductivity in $Nd_{1.85}Ce_{0.15}CuO_{4-\delta}$ is of particular interest for investigations on the electronic structure of Cu-O sheets due to its relative structural simplicity compared with other HTSC's. This offers the opportunity to study the influence of structural characteristics such as apical oxygen atoms on the dopability of HTSC's for a kind of model compound. On the other hand it is interesting to compare the simple T^* compounds to other, more sophisticated HTSC's such as, e.g., $Bi_2Sr_2CaCu_2O_{8+\delta}$, containing CuO_5 pyramids as well.

Also the comparison of the electronic properties of the *rare-earth layers* of both $Nd_{2-x}Ce_xCuO_{4-\delta}$ and $Nd_{1.4}Ce_{0.2}Sr_{0.4}CuO_{4-\delta}$ seems very promising. In the n-doped systems $M_{2-x}Ce_xCuO_{4-\delta}$ (M=Pr, Nd, Sm) there exist strong antiferromagnetic correlations between M spins[28–30] as well as antiferromagnetic order for M=Nd and Sm and $x_{Ce}=0.15$ at $T_N=1.2$ K (Refs. 31 and 32) and 4.65 K,[32,33] respectively. In the p-doped system $Nd_{1.4}Ce_{0.2}Sr_{0.4}CuO_{4-\delta}$ one could expect similar interactions between Nd spins, provided that the electronic parameters of the rare-earth sheets are similar to $Nd_{1.85}Ce_{0.15}CuO_{4-\delta}$.

The so-called "infinite-layer compound" $(Sr_{0.16}Ca_{0.84})CuO_2$, discovered in 1988 by Siegrist *et al.*,[34] was disengaged as pure infinite-layer $SrCuO_2$—in contrast to the low-pressure modification with double chains of CuO_4 tiles[35]—first in 1989 by Takano *et al.*[36] under high pressure. Superconductivity was achieved by substitution of Sr by Nd and Pr recently by Smith *et al.*[5] at a T_c of 34–40 K and by Takano *et al.* for $Sr_{1-x}Ba_xCuO_{2-\delta}$,[37] whereas for the latter compound the real composition of the superconducting phase is not yet totally clear. Up to now, Er *et al.*[38] and Korczak, Perroux, and Strobel[39] demonstrated that superconductivity also could be observed for substituting Sr by La or Sm, respectively. As is depicted in Fig. 1(d), the $Sr_{0.85}Nd_{0.15}CuO_{2-\delta}$ structure consists of planar Cu-O and Sr layers without any apical or out-of-plane oxygen positions in either of both sheets (Cu and Sr).[34] The Cu-O bond length of 1.972 Å is very similar to the n-type $Nd_{1.85}Ce_{0.15}CuO_{4-\delta}$ (1.970 Å). Therefore, one presumes this new family of HTSC's to be also an electron conductor with doped charge carriers mostly in the antibonding $d^{\sigma*}_{x^2-y^2}$ orbitals.[40–42] Recent results by Er *et al.*[43] indeed show a negative sign of the Seebeck coefficient, but unfortunately reveal a positive Hall coefficient for $x=0.1$ and $T>100$ K for the $(Sr_{1-x}La_x)CuO_{2-\delta}$ system, similar to the positive R_{Hall} of $Nd_{2-x}Ce_xCuO_{4-\delta}$ with $x \gtrsim 0.17$.[44,21] Nevertheless, confirmation of this data on other samples (e.g., thin films as prepared by Adachi *et al.*[45] and Sugii *et al.*[46]) is still lacking. From the electronic point of view therefore one may want to confirm the valence of Nd dopants to be trivalent (to get hints on the "chemical" sign of doped charge carriers) and to characterize some of the most important electronic parameters of Cu-O layers (in order to compare it with the above-mentioned prototypes of simple p- and n-type doped HTSC's).

We think photoemission spectroscopy to be a very useful tool to clarify some of the questions mentioned above because of the great success this method met with in many previous investigations on HTSC's besides other high-energy spectroscopies such as, e.g., x-ray-absorption spectroscopy or electron-energy-loss spectroscopy.[47] Furthermore, photoemission offers the possibility to determine many of the important parameters of the electronic structure by treatable theoretical models such as Anderson impurity or small-cluster calculations. After earlier publications of x-ray-photoemission-spectroscopy (XPS) data on T^* systems by Ohashi, Ikawa, and Fukunaga[48] and ourselves[49,50] we try to give here a more comprehensive study of the occupied electronic states of T^* and $Sr_{0.85}Nd_{0.15}CuO_{2-\delta}$ systems by XPS, ultraviolet-photoemission-spectroscopy (UPS), resonant photoemission, and supplementary methods such as Hall-effect and magnetic susceptibility measurements.

II. EXPERIMENTAL DETAILS

A. Sample preparation and characterization

Samples of the T^* system $Nd_{2-x-y}Ce_xSr_yCuO_{4-\delta}$, $x=0.2$, $y=0.4$, have been prepared by a standard solid-state reaction technique[51,52] using stoichiometric amounts of Nd_2O_3, CeO_2, $SrCO_3$, and CuO, each of 99.9% or higher purity. Mixed powders have been calcinated by 950 °C in air for 24 h and fired twice at 1040 °C in flowing O_2 (purity 99.998%) for 15 h with intermediate regrindings. After this, samples were again reground, pressed into pellets, and sintered twice at 1140 °C for a total of 80 h in flowing O_2. Phase purity of the samples was checked by means of x-ray diffraction in a SIEMENS D5000 diffractometer using monochromatized Cu $K\alpha_1$ radiation and a position-sensitive detector. Secondary phases with an amount of less than 5% were attributed to vestiges of the T' phase. In order to achieve superconductivity with a T_c of about 25 K an oxidation step at temperatures between 900 °C and 400 °C for more than 100 h was necessary after the final sintering procedure. Thermogravimetric-analysis (TGA) measurements did not give any hint on loading the samples with additional oxygen during this process. Thus the main purpose of

the low-temperature oxidation step might be a rearrangement of the O structure. Figure 2 shows the superconducting transition of the magnetic susceptibility [measured in a Quantum Design superconducting quantum interference device (SQUID) magnetometer model MPMS] of a representative $Nd_{1.4}Ce_{0.2}Sr_{0.4}CuO_{4-\delta}$ sample (field cooled and zero-field cooled). A Meissner fraction of more than 26% guarantees bulk nature of superconductivity.

Samples of the "infinite-layer compound" $Sr_{1-x}Nd_xCuO_{2-\delta}$ have been prepared from citrate-nitrate precursors optimized with respect to a homogeneous distribution of the corresponding cations on a molecular level. Decomposition and removal of the organics were done at temperatures around 600 °C and 1000 °C. The resulting black powders were then sintered in a modified belt press using high temperatures by simultaneously applying high quasihydrostatic pressure. Typical parameters are $T=1400$ °C and $p=40$ kbar with a second annealing step at 1100 °C and the same pressure. A slightly reducing atmosphere generated by Pt crucibles was necessary to guarantee the incorporation of Nd into the structure. The samples were then quenched down to room temperature before releasing the pressure. Samples are superconducting at a T_c^{midpoint} of about 31 K ($T_c^{\text{onset}} \approx 40$ K) with a superconducting volume fraction of $\gtrsim 26\%$ without any subsequent annealing steps necessary (Fig. 3). X-ray-diffraction patterns reveal a phase purity of more than 90% with small amounts of not yet identified high-pressure phases. The lattice parameters obtained from structure refinements are $a=3.9427$ Å and $c=3.3922$ Å.

Measurements of the lower critical field $H_{c1}^{ab}(T)$ have been performed in order to check the homogeneity of the superconducting phase. The determination of the lower critical field was done in two different ways, giving the same results for $H_{c1}^{ab}(T)$ within the error bars given in Fig. 4. The first method to obtain H_{c1}^{ab} was to determine the first deviation of the field-dependent magnetization $M(H)$ from a linear behavior or equivalently of $dM/dH|_T$ from a constant value.[53,54] A second, independent method is the determination of the magnetic field H, beyond which time-dependent relaxation in $M(H,t)$ starts.[54,32] As can be seen from Fig. 4, for both

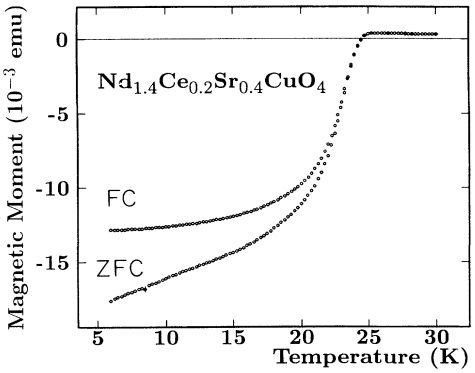

FIG. 2. Magnetic moment (field cooled and zero-field cooled) in the superconducting transition of $Nd_{1.4}Ce_{0.2}Sr_{0.4}CuO_{4-\delta}$.

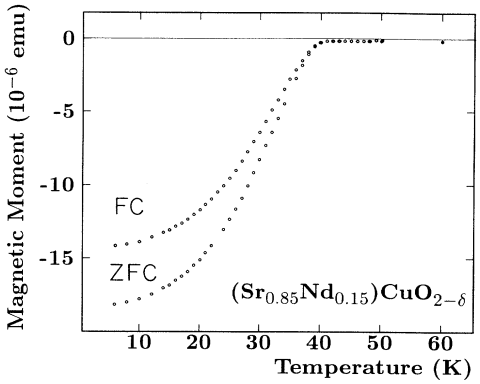

FIG. 3. Magnetic moment (field cooled and zero-field cooled) in the superconducting transition of $Sr_{0.85}Nd_{0.15}CuO_{2-\delta}$.

$Nd_{1.4}Ce_{0.2}Sr_{0.4}CuO_{4-\delta}$ and $Sr_{0.85}Nd_{0.15}CuO_{2-\delta}$ one has a parabolic temperature behavior[55] $H_{c1}^{ab}(T)=H_{c1}^{ab}(0)[1-(T/T_c)^2]$ with $(1-N)\mu_0 H_{c1}^{ab}(0)=4.4$ mT and 1.5 mT, for T^* and $Sr_{0.85}Nd_{0.15}CuO_{2-\delta}$, respectively, indicating quite good homogeneity of the superconducting phase (N denotes the demagnetization factor of the single grains of the samples).

For comparison, samples of the $Nd_{2-x}Ce_xCuO_{4-\delta}$ system have been prepared by the standard solid-state reaction technique with calcination, sintering, and reducing (Ar flow) steps following Tokura, Takagi, and Uchida[1] as described in detail in Refs. 30 and 56 for the samples used in our investigations. All samples of the $Nd_{2-x}Ce_xCuO_{4-\delta}$ system were confirmed to contain no secondary phases within the resolution of x-ray diffractometry. Superconducting samples have Meissner

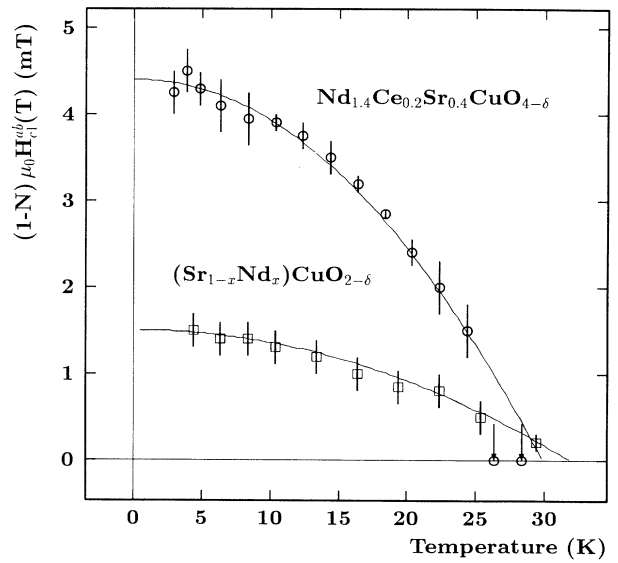

FIG. 4. Lower critical field $H_{c1}^{ab}(T)$ of $Nd_{1.4}Ce_{0.2}Sr_{0.4}CuO_{4-\delta}$ (upper curve) and $Sr_{0.85}Nd_{0.15}CuO_{2-\delta}$ (lower curve). Drawn lines are fits after $H_{c1}^{ab}(T)=H_{c1}^{ab}(0)\times[1-(T/T_c)^2]$. $Nd_{1.4}Ce_{0.2}Sr_{0.4}CuO_{4-\delta}$: $\mu_0 H_{c1}^{ab}(0)=4.4$ mT, $T_c=30$ K; $Sr_{0.85}Nd_{0.15}CuO_{2-\delta}$: $\mu_0 H_{c1}^{ab}(0)=1.5$ mT, $T_c=32$ K.

fractions of about 45% ($x_{Ce}=0.15$) and a T_c of ≈ 24 K as deduced from SQUID measurements.

For Hall-effect measurements samples were thinned to platelets with a thickness of about 0.2 mm. Gold contacts were evaporated on the samples and annealed for several hours at 400 °C in Ar or O_2 flow for T' and T^* samples, respectively. After that, wires were soldered onto the contacts using Wood's metal. The resulting resistance of the contacts was less than 0.1 Ω. Measurements were done varying the magnetic field in the way $-7\ T \rightleftharpoons 0T \rightleftharpoons 7T$ in order to rule out contributions from longitudinal resistance and magnetoresistance of sample and contacts. Values of R_H measured for various samples from different preparation batches are equal within an error of 5–10%.

B. Photoemission

XPS spectra were recorded using nonmonochromatized Al K_α radiation ($\hbar\omega=1486.6$ eV) at a base pressure of the spectrometer of 8×10^{-11} mbar. In the XPS mode the overall energy resolution of the system was about 1.0 eV. At the same spectrometer UPS measurements (He II, He I, Ne I) with a total energy resolution of about 70 meV were performed. Investigations using synchrotron radiation were done at DESY/HASYLAB, Hamburg, at the beam line E2 (spectrometer FLIPPER II), the base pressure for this apparatus being less than 1×10^{-10} with a total-energy resolution of about 0.2 eV at $\hbar\omega=100$ eV.

Clean surfaces were obtained by scraping the samples *in situ* with a coarse-grained diamond file. Scraping was repeated every 1–2 h for the reasons discussed below. After scraping, the surface quality for the XPS measurements was checked by recording the O 1*s* core line at a binding energy of $E_B=529$ eV (Fig. 5). Whereas the main feature of this line results from O^{2-} in the bulk material, the shoulder at $E_B=532$ eV is due to chemisorbed oxygen on the surface (see, e.g., Refs. 57–61), between the grain boundaries of the samples and on the sample holder. Whereas for well-scraped T' systems the 532 eV feature could not be observed any more, for the T^* compounds this feature only could be minimized to the extent shown in Fig. 5. We attribute this mainly to O adsorbates on the sample holder, which for the smaller T^* samples was also grazed by our nonfocused x-ray beam.

Besides checking the sample surface by recording the O 1*s* feature, Cu 2*p* spectra were measured for two different escape depths of photoelectrons by changing the angle between sample and x-ray source. By doing so, no change in the satellite to main line ratio could be observed for "clean" surfaces.

For measurements of the valence-band chemisorbed oxygen on the surface is indicated by a peak at $E_B=9.5$ eV in the spectra, as was also observed for many other divalent oxocuprates.[62–64,58,25] The evolution of this feature for a freshly scraped surface of $Nd_{1.4}Ce_{0.2}Sr_{0.4}CuO_{4-\delta}$ after several times under UHV at room temperature can be seen from Fig. 6. A similar behavior was also observed for the other compounds under investigation. Together with an increase of the 9.5-eV peak the relative weights of the two main features of the valence band at 3.2 eV and 4.8 eV also change, as can be seen from Fig. 6, too.

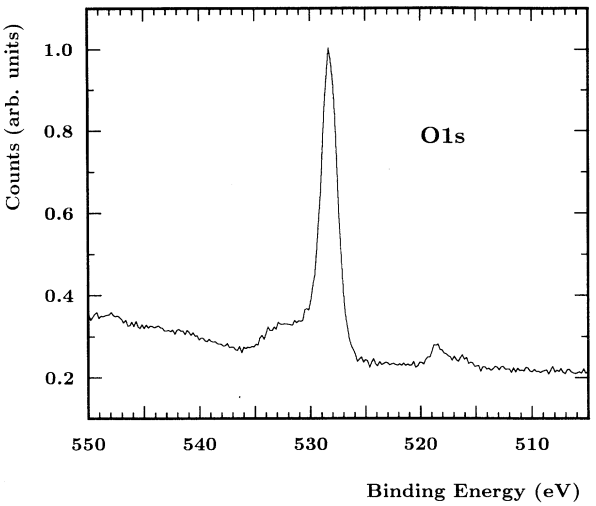

FIG. 5. O 1*s* peak of $Nd_{1.4}Ce_{0.2}Sr_{0.4}CuO_{4-\delta}$ after scraping under UHV.

Because of the rapid surface degradation at room temperature for metallic and superconducting samples, a Fermi edge could not be observed, as it was detected by room-temperature XPS by Suzuki *et al.*[65] and Sakisaka *et al.*[66] in the case of $Nd_{1.85}Ce_{0.15}CuO_{4-\delta}$. This indicates the topmost surface region of the samples to have a slightly changed oxygen content compared to the metallic material. Oxygen depletion of the uppermost layers of the structure only could be avoided by cooling the samples down to 10–20 K and scraping or cleaving the *cooled samples,* as was done for T' single crystals, e.g., by Allen *et al.*[67] Further consequences from this surface behavior will be discussed further below.

All core-level and valence-band spectra for each compound were recorded for several samples from different

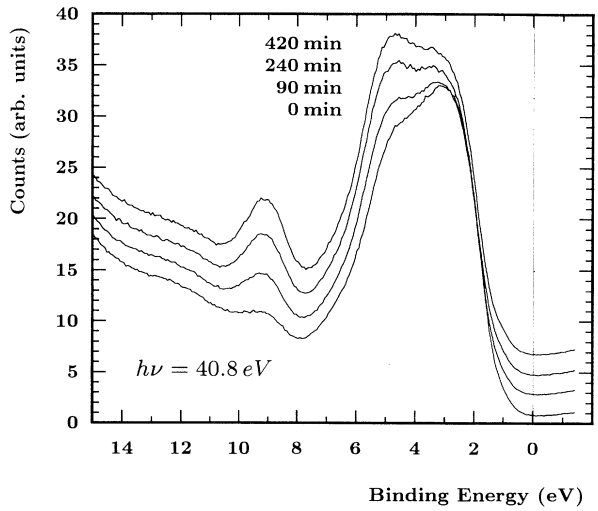

FIG. 6. Surface degradation of $Nd_{1.4}Ce_{0.2}Sr_{0.4}CuO_{4-\delta}$ valence-band spectra after various times under UHV (1×10^{-10} mbar) at room temperature.

preparation batches. For well-characterized surfaces differences between various samples of the same compound could not be observed within our experimental resolution.

III. RESULTS AND DISCUSSION

A. Copper-oxygen layers

Many theoretical and summarizing articles have discussed the importance of the apical oxygen atoms and the Cu-O bond length for the dopability of HTSC's. Discussions in terms of ligand field splitting,[41,42] Madelung energies,[68,69] and band-structure calculations[70] have been given to explain the reasons for different signs of charge carriers in superconducting cuprates of T and T^* structure on the one hand and T' compounds on the other. We try to work out the differences and similarities of the electronic structure of the closely related $Nd_{1.4}Ce_{0.2}Sr_{0.4}CuO_{4-\delta}$ and $Nd_{2-x}Ce_xCuO_{4-\delta}$ systems as well as of the infinite-layer $Sr_{0.85}Nd_{0.15}CuO_{2-\delta}$ in order to find a criterion for the dopability of high-T_c cuprates from the point of view of high-energy spectroscopy.

1. Cu 2p core-level spectra

Figure 7 depicts the Cu $2p_{3/2}$ core-level spectra for oxidized (superconducting) and nonoxidized $Nd_{1.4}Ce_{0.2}Sr_{0.4}CuO_{4-\delta}$ as well as, for comparison, of calcined Nd_2CuO_4. Calcined Nd_2CuO_4 has been chosen as a reference since, as a previous investigation showed,[26] Cu $3d$ occupancy is enhanced by Ce doping of T' compounds[25,64,71,72] as well as by heat treatment of the samples ($T \gtrsim 1050\,^\circ$C), which is indicated by an enhanced relative intensity of the main line at $E_B = 933$ eV. For calcined Nd_2CuO_4 we therefore expect no enhanced Cu $3d$ occupancy due to oxygen vacancies and thus no "Cu^+" contribution to the Cu $2p$ spectra.

Similar to all other cuprate HTSC's the existence of a main line at $E_B = 933$ eV and a broad satellite around 942 eV in the Cu $2p_{3/2}$ spectra indicates Cu to be mainly in a divalent oxidation state. The reason for the existence of an additional satellite in Cu^{2+} compounds was first discussed for Cu dihalides by Larsson[73] and Sawatzky and co-workers:[74,75] The satellite feature mainly results from a $|d^9\underline{c}\rangle$ configuration in the final state of the photoemission process ($\underline{c}$ denotes a hole in the Cu $2p$ core level). It consists of eight single lines due to the coupling of the angular momenta of the core hole ($J=\frac{3}{2}$) and of the open d shell ($J=\frac{5}{2}$ *and* $J=\frac{3}{2}$, since for strong crystal fields the total angular momentum is not a good quantum number any more). The main line at 933 eV is predominantly due to a charge-transfer process from O $2p$ levels into the open Cu $3d$ shell in the final state. Since in the presence of a core hole in the Cu $2p$ shell the Cu $3d$ levels are energetically lowered by an attractive core-hole potential U_{dc} the above-mentioned charge transfer becomes more probable. According to its derivation the main line is denoted as $|d^{10}\underline{L}\underline{c}\rangle$, $\underline{L}$ being a hole in the O $2p$ (ligand) orbital.

From Fig. 7 one can see the relative weight of the main line for Nd_2CuO_4 to be noticeably higher than for the two

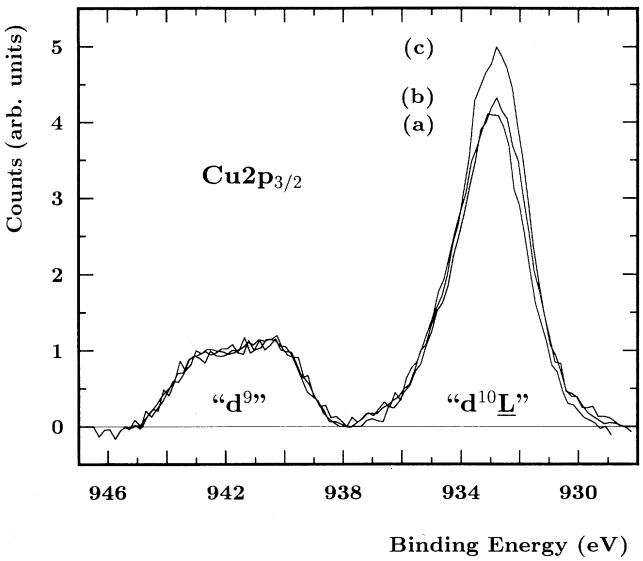

FIG. 7. Cu $2p_{3/2}$ core-level spectra of oxidized (a) and nonoxidized (b) $Nd_{1.4}Ce_{0.2}Sr_{0.4}CuO_{4-\delta}$ as well as of Nd_2CuO_4 (c). Spectra are normalized onto the $|d^9\underline{c}\rangle$ satellite.

$Nd_{1.4}Ce_{0.2}Sr_{0.4}CuO_{4-\delta}$ samples, whereas the peak positions are essentially the same for both systems. Between the superconducting (oxidized) T^* sample and its nonoxidized counterpart there is only a very small difference in the intensity ratio of no more than 5%. This perhaps might be interpreted as a removal of some remainders of "monovalent" copper (a diminution of Cu $3d$ occupancy in the sense of Refs. 25 and 26) due to the oxidation treatment.

For a theoretical description of the Cu $2p_{3/2}$ spectra we take a single-impurity Anderson model[76–79] as will be briefly described in the following.

In the sudden approximation one has for the photoemission spectrum $I(E_{\rm kin})$, applying Fermi's golden rule,

$$I(E_{\rm kin}) \sim \sum_j |\langle f_j|c|0\rangle|^2 \delta(E_{\rm kin}-(\varepsilon_0-\varepsilon_f^j+\hbar\omega)) \quad (1)$$

or, rewriting the δ distribution,

$$I(E_{\rm kin}) \sim \lim_{\delta\to 0} {\rm Im}G(E_{\rm kin}-i\delta)\ , \quad (2)$$

with

$$G(z) \equiv \left\langle 0 \left| c^\dagger \frac{1}{z-\varepsilon_0-\hbar\omega+H_f} c \right| 0 \right\rangle\ , \quad (3)$$

where $|f_j\rangle$ and $|0\rangle$ denote final states and initial (ground) state, respectively, and ε_f^j and ε_0 the corresponding energies of the system. c creates a photoemission hole in the system and H_f stands for the Hamiltonian of the final state.

Defining the Anderson single-impurity Hamiltonian as[80]

$$H = \sum_{\rm k} \varepsilon_{\rm k} c_{\rm k}^\dagger c_{\rm k} + \varepsilon_d d^\dagger d + \sum_{\rm k} (t_{\rm k} c_{\rm k}^\dagger d + {\rm H.c.}) + U_{dd} n_d - U_{dc} n_d (1-n_c) \quad (4)$$

($\varepsilon_{\mathbf{k}}, c_{\mathbf{k}}^{\dagger}$ are the energies and creation operators of the O $2p$ band; ε_d, $d^{\dagger}$ are the energy and creation operator of the Cu $3d$ level; $t_{\mathbf{k}}$ is the Cu-O hybridization; U_{dd} is the Cu $3d$ Coulomb correlation energy), one has to calculate the ground-state Green's function of the final state, giving

$$\langle 0|G(z)|0\rangle = \frac{1}{z-\varepsilon_0} + \frac{1}{(z-\varepsilon_0)^2} \frac{\langle n_d\rangle_0 U_{dc}}{1-U_{dc}\langle d|G_0(z)|d\rangle} , \tag{5}$$

with

$$\langle d|G_0(z)|d\rangle = \left[z - \sum_{\mathbf{k}} \frac{t_{\mathbf{k}}^2}{z-\epsilon_{\mathbf{k}}} \right]^{-1} . \tag{6}$$

The ground-state energy ε_0 and ground-state d occupancy $\langle n_d\rangle_0$ can be obtained from the Green's function of the initial state, given by Eq. (6). For the energy dispersion of the O $2p$ band in Eq. (4) we adopt a simple two-dimensional tight-binding relation

$$\varepsilon_{\mathbf{k}} = \bar{\varepsilon}_{\mathbf{k}} - \frac{W}{4}[\cos(k_x a) + \cos(k_y a)] \tag{7}$$

and an energy-dependent hybridization

$$t_{\mathbf{k}} \equiv t(\varepsilon_{\mathbf{k}}) = \frac{2t_0}{45N} \sqrt{1-(\varepsilon_{\mathbf{k}}-\bar{\varepsilon}_{\mathbf{k}})^2/(W/2)^2} , \tag{8}$$

with $N=3600$ **k** states. In this model we disregard all other Cu $3d$ states besides $3d_{x^2-y^2}$ (b_1 symmetry) as well as the coupling of angular momenta of the core hole and open d shell, resulting in the absence of any multiplet splitting of the $|d^9\underline{c}\rangle$ satellite. A more careful analysis taking into account also the other Cu $3d$ orbitals a_1, b_2, and $2\times e$ besides b_1, a symmetry-dependent Cu-O hybridization, and the effects of multiplet splitting can be found, e.g., in Refs. 81 or 82. Also we should refer to the Cu $2p$ XPS model calculation of Tranquada *et al.*[83] for CuO_6 and CuO_{12} clusters, including also Cu $4s$ and $4p$ states in the final-state screening process.

We also neglect "Cu^{3+}" initial states due to doped holes in the initial- and final-state calculations. Because of the large Coulomb correlation energy at the copper site, the $3d^8$ configuration only contributes to a negligible extent to initial and final states.[84] Therefore neither the main line to satellite intensity ratio nor the peak separation should be significantly influenced by hole doping.[85]

In our case we are interested in extracting leads for the Cu-O hybridization t_0 and the charge-transfer energy $\tilde{\Delta} \equiv \varepsilon_d - \bar{\varepsilon}_{\mathbf{k}} + U_{dd}$. The core-hole potential U_{dc} is left as a free parameter like the O $2p$ bandwidth W, for which band-structure calculations on $Nd_{1.85}Ce_{0.15}CuO_{4-\delta}$ (Refs. 86 and 87) and T^*-type Nd_2CuO_4 (Ref. 88) give values of about 4–6 eV.

Table I gives the values for energy separation ΔE and intensity ratio I_m/I_s of main line and satellite for Nd_2CuO_4, $Nd_{1.4}Ce_{0.2}Sr_{0.4}CuO_{4-\delta}$, and $Bi_2Sr_2CaCu_2O_{8+\delta}$ (as from Ref. 59 obtained at the same XPS spectrometer). ΔE was determined from the energy difference of the $|d^{10}\underline{L}c\rangle$ peak and the center of gravity of the $|d^9\underline{c}\rangle$ feature.

TABLE I. Values for main line to satellite intensity ratio I_m/I_s and energy difference ΔE obtained from Cu $2p_{3/2}$ core-level spectra.

	Nd_2CuO_4	$Nd_{1.4}Ce_{0.2}Sr_{0.4}CuO_{4-\delta}$	$Bi_2Sr_2CaCu_2O_{8+\delta}$ [a]
I_m/I_s	3.1	2.6	2.2
ΔE (eV)	8.7	8.6	8.6

[a]Reference 59.

We are analyzing only the Cu $2p_{3/2}$ spectra since for the Cu $2p_{1/2}$ part interference effects between the relaxation of valence electrons and the Costers-Kronig decay of the $2p_{1/2}$ core hole are known to change the satellite to main line ratio to a non-negligible extent.[89,90]

Figures 8(a) and 8(b) show t_0 and $\tilde{\Delta}$, respectively, as a function of the O $2p$ bandwidth W for Nd_2CuO_4, $Nd_{1.4}Ce_{0.2}Sr_{0.4}CuO_{4-\delta}$, and $Bi_2Sr_2CaCu_2O_{8+\delta}$ [$U_{dc}=8.2$ eV (Ref. 91)]. All curves saturate for small values of W onto a constant value (zero bandwidth limit of a 2×2 configuration interaction model[74]) and approach each other for higher values of W. Figures 9(a) and 9(b) depict the values obtained for t_0 and $\tilde{\Delta}$ for varying U_{dc} between 8 eV and 9 eV at a constant $W=4$ eV. In all four diagrams the values of T^*-type $Nd_{1.4}Ce_{0.2}Sr_{0.4}CuO_{4-\delta}$ lie between the parameters for Nd_2CuO_4 and $Bi_2Sr_2CaCu_2O_{8+\delta}$. We assume this trend in the Cu-O hy-

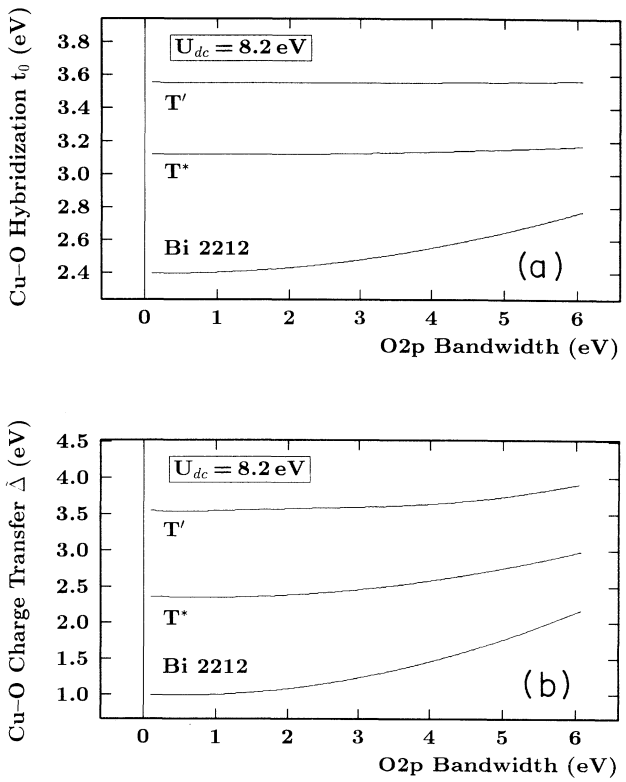

FIG. 8. Cu-O hybridization t_0 (a) and charge-transfer energy $\tilde{\Delta}$ (b) as a function of O $2p$ bandwidth W for a constant $U_{dc}=8.2$ eV (see text for definitions).

TABLE II. Cu-O bond lengths for Nd_2CuO_4, $Nd_{1.4}Ce_{0.2}Sr_{0.4}CuO_{4-\delta}$, and $Bi_2Sr_2CaCu_2O_{8+\delta}$.

	Nd_2CuO_4	$Nd_{1.4}Ce_{0.2}Sr_{0.4}CuO_{4-\delta}$	$Bi_2Sr_2CaCu_2O_{8+\delta}$
Cu-$O^{\text{in plane}}$ (Å)	1.97	1.94	1.95
Cu-O^{apex} (Å)		2.23	3.13
Reference	92	7	93

bridization to be mainly due to the existence of a remote apical oxygen in T^* and $Bi_2Sr_2CaCu_2O_{8+\delta}$ compounds, which lowers the *mean* Cu-O overlap for the *p*-doped compounds. Values for the Cu-O distances in the three systems under consideration are listed in Table II. For a rough estimate of the mean value of t_0 we use Harrison's rules[94] for the distance dependence of $3d$-$2p$ hybridization and take the mean over the Cu $3d$-O $2p$ bonds listed in Table III. For $Nd_{1.4}Ce_{0.2}Sr_{0.4}CuO_{4-\delta}$ and $Bi_2Sr_2CaCu_2O_{8+\delta}$ we thus estimate t_0 to be lower by about 10% and 25% compared to Nd_2CuO_4, respectively. This could account for the experimental findings for $W \gtrsim 4$ eV and $U_{dc} \gtrsim 8.2$ eV [Figs. 8(a) and 9(a)].

The difference in the charge-transfer energies $\tilde{\Delta}$ of *n*- and *p*-type systems could with some caution be explained by an enhanced Cu $3d$ Coulomb correlation energy U_{dd} in Eq. (4) for the *n*-type Nd_2CuO_4: Because of the missing apical oxygen two charge carriers on the Cu site are not allowed to delocalize as good as for the compounds containing CuO_5 pyramids. We will refer to this interpretation further below in the discussion of the valence-band spectra.

Because of the simplifications of the used model, as already mentioned above, and because of the uncertainties in determining ΔE and I_m/I_s, the absolute values obtained for $\tilde{\Delta}$ and t_0 should not be taken too serious. Also one should bear in mind that together with changes in $\tilde{\Delta}$ also changes in U_{dc} are going along, described by the empirical relation $U_{dc} \simeq 0.7 U_{dd}$.[79] Thus the given results only should be interpreted as to give some general trends for hybridization and charge-transfer energy.

Explicit values for the Coulomb correlation energy U_{dd} unfortunately cannot be obtained directly from the Cu $2p$ core-level spectra. A way to give a crude estimate of U_{dd} is to consider the Cu L_3 vv Auger line and its relative position to the self-convolution of the partial Cu $3d$ valence band by the relation[95]

$$U_{dd}^{\text{eff}} \approx E_B(\text{Cu } 2p) - 2E_B(v) - E_{\text{kin}}(L_3vv) \, . \tag{9}$$

$E_B(\text{Cu}2p)$, $2E_B(v)$ and $E_{\text{kin}}(L_3vv)$ denote the binding energies of a Cu $2p_{3/2}$ core hole and two noncorrelated Cu $3d$ holes (two-hole binding energy) as well as the energy of the Cu L_3vv Auger line. The quantity $2E_B(v)$ should be determined from the self-convolution of the XPS valence band.[96] The line shape and position of the Auger line are strongly influenced by the multiplet structure of the valence band,[95,97] the Coster-Kronig decay of a Cu $2p_{1/2}$ core hole[98] as well as by the relaxation of the two-hole final state of the Auger process.[99] Therefore this procedure only can give an effective and very rough estimate for the Coulomb correlation energy. Keeping in mind this proviso, one obtains values for U_{dd}^{eff} of 7.5 eV and 7.2 eV for $Nd_2CuO_{4-\delta}$ and $Nd_{1.4}Ce_{0.2}Sr_{0.4}CuO_{4-\delta}$, respectively, which is considerably larger than the value of $U_{dd}^{\text{eff}}=6$ eV obtained by Hillebrecht *et al.* for $Bi_2Sr_2CaCu_2O_{8+\delta}$.[100]

TABLE III. Parameters for Cu-O hybridization and charge-transfer energies used in the valence-band cluster model.

	Cu $3d$	t_{pd}^{i} [a]	$\epsilon_{p,i}$ [a]	$\epsilon_{d,i}$
$a_1^{\text{in plane}}$	$d_{3z^2-r^2}$	t_{pd}^{σ}	$\Delta+t_{pp}$	0
a_1^{apex}		$\sqrt{2}t_{pd}^{\sigma}v^{3.5}$ [b]	Δ	
b_1	$d_{x^2-y^2}$	$\sqrt{3}t_{pd}^{\sigma}$	$\Delta-t_{pp}$	0
b_2	d_{xy}	$2t_{pd}^{\pi}$	$\Delta+t_{pp}$	0
$e^{\text{in plane}}$	d_{xz},d_{yz}	$\sqrt{2}t_{pd}^{\pi}$	Δ	0
e_{apex}		$\sqrt{2}t_{pd}^{\pi}v^{3.5}$ [b]	Δ	

[a]Reference 108.
[b]$v \equiv d_{\text{in plane}}^{\text{Cu-O}}/d_{\text{apex}}^{\text{Cu-O}}$.

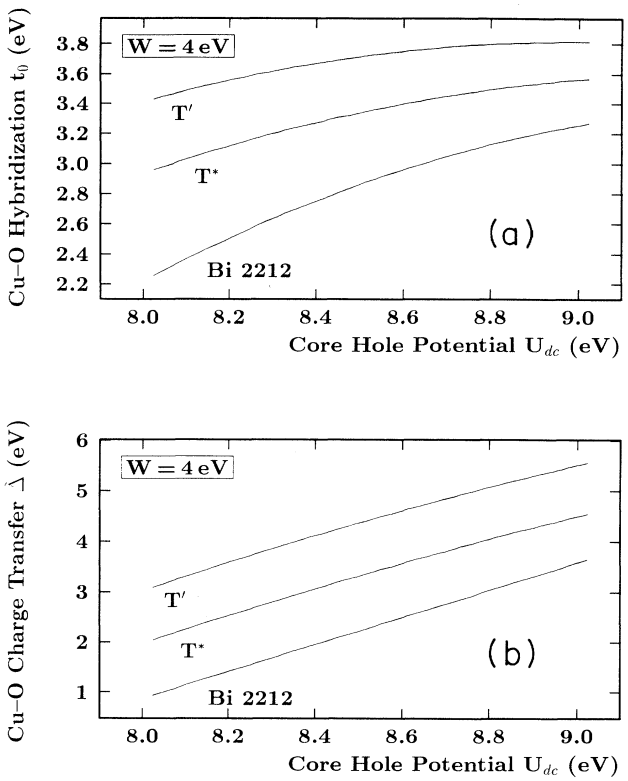

FIG. 9. Cu-O hybridization t_0 (a) and charge-transfer energy $\tilde{\Delta}$ (b) as a function of the core-hole potential U_{dc} for a constant O $2p$ bandwidth $W=4$ eV.

2. *Valence-band spectra*

Figure 10 depicts the valence-band spectra of $Nd_{1.85}Ce_{0.15}CuO_{4-\delta}$ and $Nd_{1.4}Ce_{0.2}Sr_{0.4}CuO_{4-\delta}$ recorded with He II light ($\hbar\omega = 40.8$ eV). As for all other cuprate HTSC's,[101] the main valence band consists of two features around the binding energies of 3.2 eV and 4.8 eV, respectively. From the characteristic photon energy dependence of both features between $\hbar\omega = 20$ eV and 100 eV (not shown here) one can attribute predominant Cu (O) character to the feature at lower (higher) binding energy.[102] For comparison, the calculated total and partial Cu density of states (DOS) from local-density-approximation (LDA) calculations for T^*-type Nd_2CuO_4 by Szotek, Guo, and Temmerman[88] are also shown. In order to get a crude correspondence between the LDA-DOS and the experimental spectra one has to shift the theoretical curve by about 1.6 eV towards higher binding energies, indicating again both the importance of electron correlations[103] also in the $Nd_{1.4}Ce_{0.2}Sr_{0.4}CuO_{4-\delta}$ system as well as the degradation of the surface for room-temperature measurements on T^* samples (see, e.g., Refs. 63 and 67). Comparison of the He II valence-band spectra of $Nd_{1.85}Ce_{0.15}CuO_{4-\delta}$ and $Nd_{1.4}Ce_{0.2}Sr_{0.4}CuO_{4-\delta}$ shows an increased spectral weight of the valence band of T^* at low binding energies, which we will discuss in terms of a simple cluster approach further below.

Valence-band spectra in the Cu^{2+} ($3p \rightarrow 3d$) resonance at $\hbar\omega = 74$ eV can be seen from Figs. 11(a) and 11(b) for $Nd_{1.4}Ce_{0.2}Sr_{0.4}CuO_{4-\delta}$ and Nd_2CuO_4 as well as for $Sr_{0.85}Nd_{0.15}CuO_{2-\delta}$ in Fig. 11(c). Arrows indicate the resonantly enhanced Cu $3d^8$ singlet final states (^1G) at about 13 eV. The resonance mechanism is attributed to a

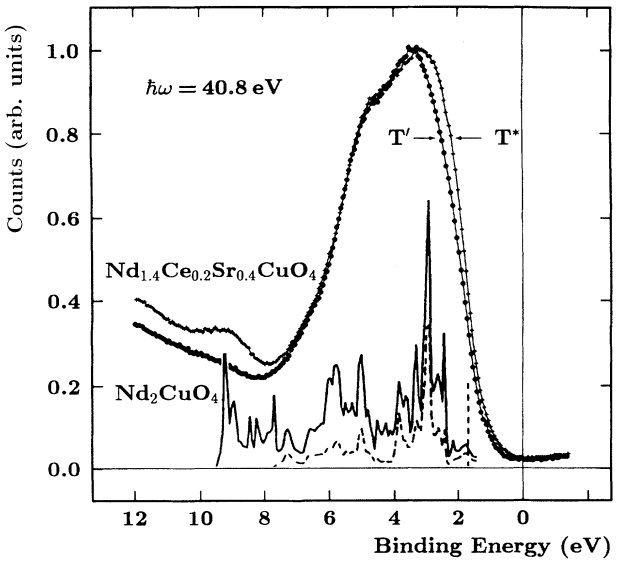

FIG. 10. He II valence-band spectra ($\hbar\omega = 40.8$ eV) of Nd_2CuO_4 and $Nd_{1.4}Ce_{0.2}Sr_{0.4}CuO_{4-\delta}$ (solid line). For comparison, the total and partial Cu DOS obtained from LDA band-structure calculations (Ref. 88) are depicted, too (solid line, total DOS, dashed line, partial Cu DOS). Note the different positions of the Fermi energy.

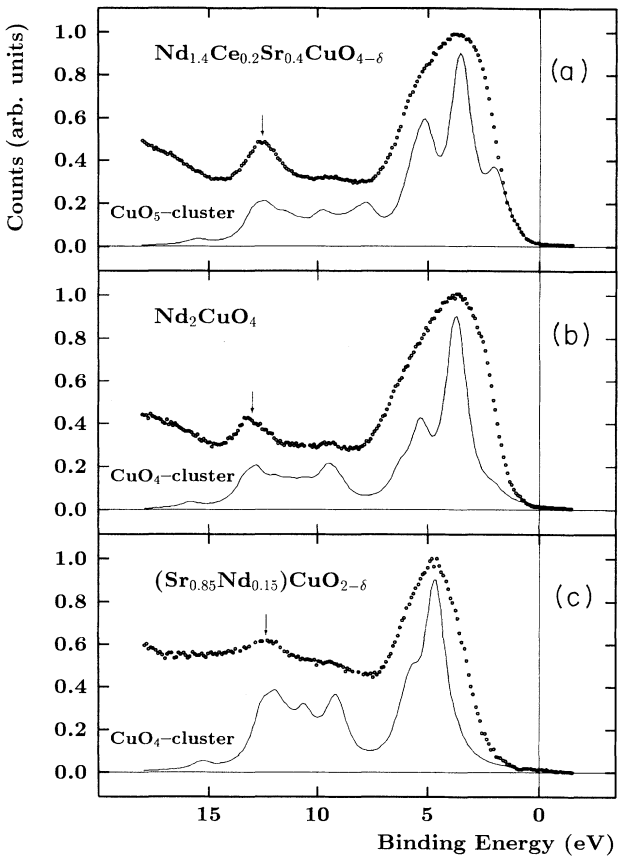

FIG. 11. Valence-band spectra of $Nd_{1.4}Ce_{0.2}Sr_{0.4}CuO_{4-\delta}$ (a), Nd_2CuO_4 (b), and $Sr_{0.85}Nd_{0.15}CuO_{2-\delta}$ (c) in the Cu $3p \rightarrow 3d$ resonance at $\hbar\omega = 74$ eV together with the partial Cu $3d$ valence-band spectra obtained from CuO_4 (T', ∞) and CuO_5 (T^*) cluster calculations (for parameters, see Table IV).

constructive interference of the normal $3d$ emission and the Auger decay of a $3p \rightarrow 3d$ excited Cu $3p$ electron

$$3p^6 3d^9 \xrightarrow{\hbar\omega} 3p^5 3d^{10} \rightarrow 3p^6 3d^8 + e^- \ .$$

For the $3d^8$ triplet final states around ≈ 9 eV one has a considerably lower value of the matrix element for the Auger decay of $3p^5 3d^{10}$,[104] which is why this feature cannot be seen as well in the spectra.

As can be seen from Figs. 11(a) and 11(b), the main difference between T' and T^* compounds seems to be a shift of the $3d^8$ singlet feature towards lower binding energies for the p-doped compound. This was observed also for $Bi_2Sr_2CaCu_2O_{8+\delta}$ in comparison with the n-doped T' systems by Grassmann *et al.*[25] For $Sr_{0.85}Nd_{0.15}CuO_{2-\delta}$, the main valence band is considerably narrower and the energy position of the resonantly enhanced $3d^8$ feature is shifted even further towards lower values of E_B.

An interpretation of these results is done within a simple CuO_4^{6-} cluster model with $D4h$ symmetry in the case of Nd_2CuO_4 and $Sr_{0.85}Nd_{0.15}CuO_{2-\delta}$, as was given by Eskes, Tjeng, and Sawatzky for CuO.[105,106] For the

$Nd_{1.4}Ce_{0.2}Sr_{0.4}CuO_{4-\delta}$ compounds we employ a CuO_5 cluster with $C4v$ symmetry,[102] taking into account the apical oxygen of the T^* structure. In the following we will give a short description of the model.

With the Hamiltonian for the $CuO_n^{(2n-2)-}$ cluster

$$H=\sum_i \varepsilon_{d,i} d_i^\dagger + \sum_i \varepsilon_{p,i} c_i^\dagger c_i + \sum_i (t_{pd}^i d_i^\dagger c_i + \text{H.c.}) + \sum_{klmn} U_{klmn} d_k^\dagger d_l d_m^\dagger d_n \quad (10)$$

($\epsilon_{d,i}$ and $\epsilon_{p,i}$ are the energies of the Cu $3d$ and O $2p$ levels, respectively; indices of the sums denote summation over the four symmetries a_1, b_1, b_2, and e, involved in $D4h$ and $C4v$; Coulomb interactions on the O site and between O $2p$ and Cu $3d$ electrons are not taken into account), one can calculate the ground-state configuration [in which due to the large crystal-field (CF) and ligand-field splitting of the ground state only orbitals with b_1 symmetry are regarded ($d_{x^2-y^2}$ and p_{b1})] and the partial Cu $3d$ photoemission spectrum from Eq. (3):

$$I(E)\sim \lim_{\delta\to 0^>} \sum_{mn}\sum_{i,j} \langle 0|d_m^\dagger|i\rangle \left\langle i\left|\frac{1}{E-i\delta-\epsilon_0+H_f}\right|j\right\rangle \times \langle j|d_n|0\rangle , \quad (11)$$

m and n denoting again the symmetries and i,j being final states of the photoemission process.

As described in detail in Ref. 105, we adopt for the symmetry-dependent hybridizations and O $2p$ energies the values given in Table III.

For the CuO_5 cluster we additionally adopt a hybridization between *in-plane* and *apex* O $2p$ orbitals of the same symmetry,[105] namely,

$$\begin{cases} -\sqrt{2}t_{pp}\dfrac{v^3}{(1+v^2)^2} & \text{for } a_1 , \\ t_{pp}\dfrac{v^3}{(1+v^2)^2} & \text{for } e . \end{cases} \quad (12)$$

The Coulomb correlation matrices U_{klmn} are given in terms of the Racah parameters A, B, and C (Refs. 108 and 109) explicitly, e.g., in Ref. 105 for the $D4h$ point group, and are found to be the same for $C4v$ symmetry. For B and C we take the free-ion values given in Ref. 110, namely, $B=0.15$ eV and $C=0.58$ eV, whereas the main diagonal term of the Coulomb correlation A is left as a free parameter.

Table IV gives the parameters of the theoretical spectra to be seen in Figs. 11(a)–11(c), which are broadened with a Lorentzian of 1.0 eV full width at half-maximum (FWHM).

Keeping in mind the uncertainties in determining exact-fit parameters for the spectra and the simplicity of the model used here (in contrast to more sophisticated descriptions with larger clusters such as Cu_2O_7,[111] Anderson impurity models,[112] or including also Cu $4s$ states[113]) from the energy position of the $3d^8$ satellite ($^1A_2$ symmetry in terms of the cluster model) one obtains for the T^* system a remarkably lower value for the Coulomb correlation energy A [and thereby of Δ (Ref. 114)]. This is also confirmed by the results from Cu $2p$ spectra and Auger data, given above. The value of $U_{dd}(^1G)=A+4B+2C=7.8$ eV for T^* is considerably larger than the correlation energy of $U_{dd}=6.5$ eV found by Shen *et al.*[115] for La_2CuO_4 by means of a 3×3 configuration interaction model for the valence-band spectra.

TABLE IV. Parameters used for the Cu $3d$ valence-band cluster calculations (Fig. 11). For definitions, see text.

	$Nd_{1.4}Ce_{0.2}Sr_{0.4}CuO_{4-\delta}$	Nd_2CuO_4	$Sr_{0.85}Nd_{0.15}CuO_{2-\delta}$
A (eV)	6.00	6.70	6.70
t_{pd}^σ (eV)	1.40	1.40	1.00
t_{pd}^π (eV)	0.61	0.61	0.44
Δ (eV)	2.20	2.75	2.75
t_{pp} (eV)	1.00	1.00	0.50
v[a]	0.87		
n_{d0}	0.38	0.33	0.23
ϵ_0 (eV)	−1.90	−1.70	−0.94

[a] $v\equiv d_{\text{in plane}}^{\text{Cu-O}}/d_{\text{apex}}^{\text{Cu-O}}$.

For Cu-O and O-O hybridization there is no necessity for changing the values between $Nd_{1.4}Ce_{0.2}Sr_{0.4}CuO_{4-\delta}$ and Nd_2CuO_4. Please note that changes in the Cu-O hybridization as obtained from the Cu $2p$ Anderson impurity calculations are mainly due to a change of the overlap between Cu and the apex oxygen, which has not been treated separately for the evaluation of the core-level spectra.

For the CuO_5 cluster calculation as done for $Nd_{1.4}Ce_{0.2}Sr_{0.4}CuO_{4-\delta}$ we furthermore obtain an enhanced spectral weight at the lower-energy side of the main valence band due to split-off $^3B_1$ states. This is in good agreement to the observations for the higher-resolution He II spectra mentioned above (Fig. 10). We therefore do not attribute the observed differences to any kind of shift of E_F by doping holes or electrons, as should be expected in rigid-band descriptions.

For the "infinite-layer" compound $Sr_{0.85}Nd_{0.15}CuO_{2-\delta}$ we obtain (besides a comparatively high value of $U_{dd}=6.7$ eV as in the case of Nd_2CuO_4) considerably diminished Cu-O and O-O hybridizations. This behavior cannot be understood in terms of the Cu-O bond lengths in both compounds [Nd_2CuO_4, 1.970 Å (Ref. 92); $Sr_{0.85}Nd_{0.15}CuO_{2-\delta}$, 1.972 Å (Ref. 5)]. One could explain this either by a very high number of oxygen vacancies in the Cu-O layers, reducing the *mean* Cu-O overlap, or by a very different overall charge density in the cuprate sheets of $Sr_{0.85}Nd_{0.15}CuO_{2-\delta}$. A hint on an altered hybridization between Cu and O also could be seen in recent results of Wooten *et al.*[116] on the pressure dependence of the critical temperature $T_c(p)$ of the infinite-layer compound. Their experiments give a totally different behavior of $T_c(p)$ compared to the T' systems.[117] Furthermore, it should be mentioned that also for the nonsuperconducting $Ca_{0.85}Sr_{0.15}CuO_2$ compound with its small Cu-O bond length d of 1.93 Å (Ref. 118)

Tranquada *et al.*[84] observed values comparable to those of Nd_2CuO_4 with $d=1.97$ Å.

From the results given above we presume the high value of the Cu $3d$ Coulomb repulsion (which we attribute to a diminished screening of the d^8 final-state configuration) to be a characteristic feature of electron-dopable high-T_c cuprates. We suppose the high U_{dd} in T' and infinite-layer compounds to prevent doped electrons to remain localized at the Cu sites. Reduced screening and thus a higher U_{dd} can be achieved either by a smaller number of ligand oxygen atoms ($La_2CuO_4 \leftrightarrow Nd_2CuO_4$) or by an elongated Cu-O bond length (lower Cu-O hybridization). Former investigations[119] showed that in the series of T' compounds $M_{1.85}Ce_{0.15}CuO_{4-\delta}$ with M=Pr,Nd,Sm the intra-atomic Coulomb repulsion is diminished with decreasing Cu-O bond length [Pr→Nd→Sm (→Eu→Gd)], being in square with Gd_2CuO_4 not to become an n-doped HTSC any more. The very low Cu-O hybridization for the $Sr_{0.85}Nd_{0.15}CuO_{2-\delta}$ compound thus makes electron doping even more favorable by a reduced screening of the d^8 configuration at the copper site and/or by a diminished splitting of bonding $d^{\sigma}_{x^2-y^2}$ and antibonding $d^{\sigma*}_{x^2-y^2}$ orbitals (following the arguments of Goodenough and Manthiram in Refs. 41 and 42).

3. *Hall-effect measurements on $Nd_{1.4}Ce_{0.2}Sr_{0.4}CuO_{4-\delta}$*

Neither from Cu $2p$ nor from valence-band photoemission spectra could be observed any significant change between superconducting and nonsuperconducting samples of $Nd_{1.4}Ce_{0.2}Sr_{0.4}CuO_{4-\delta}$. This might be due to the changed oxygen stoichiometry of the samples' surface as mentioned above. In order to clarify the importance of the final oxygen treatment of $Nd_{1.4}Ce_{0.2}Sr_{0.4}CuO_{4-\delta}$ samples a little more, we performed Hall-effect measurements on oxidized (superconducting) and nonoxidized samples, as is shown in Fig. 12. For superconducting $Nd_{1.4}Ce_{0.2}Sr_{0.4}CuO_{4-\delta}$ our results are in good agreement with those obtained by Kosuge *et al.*[19] The temperature behavior of the absolute values $|R_H(T)|$ closely resembles this of n-doped $Nd_{1.85}Ce_{0.15}CuO_{4-\delta}$,[2,56,21] indicating a further striking symmetry between those two n- and p-doped HTSC's.

The Hall coefficient of the nonoxidized $Nd_{1.4}Ce_{0.2}Sr_{0.4}CuO_{4-\delta}$ samples is found to be by about one order of magnitude larger than for the superconducting system. Within a simple one-band model—which is surely not appropriate for HTSC compounds[120]—this would mean an enhanced occupation of the conduction-band states by doped holes becoming intrinsic due to the low-temperature oxygen treatment of the samples or—within a two-band description—an enhanced mobility of the positive majority-charge carriers.

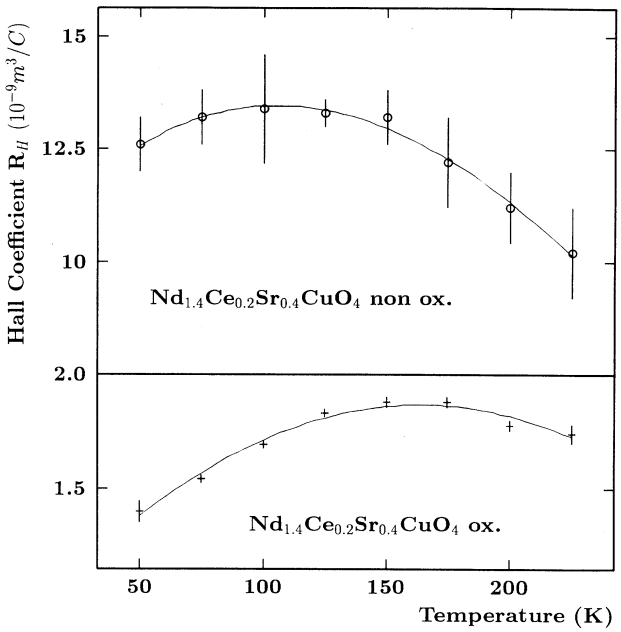

FIG. 12. Hall coefficient $R_H(T)$ of oxidized (lower part) and nonoxidized (upper part) $Nd_{1.4}Ce_{0.2}Sr_{0.4}CuO_{4-\delta}$.

B. Rare-earth layers

1. *$Nd_{1.4}Ce_{0.2}Sr_{0.4}CuO_{4-\delta}$ systems*

In the n-doped $M_{2-x}Ce_xCuO_{4-\delta}$ systems the rare-earth layers are of particular interest not only due to their role as charge-carrier reservoir but also for their magnetic properties. Besides large antiferromagnetic correlations of rare-earth spins in the case of M=Nd and Sm antiferromagnetic order occurs below $T=1.2$ K and $T=4.65$ K, respectively. In the $Nd_{1.4}Ce_{0.2}Sr_{0.4}CuO_{4-\delta}$ systems at least one of the two Nd-O sheets in the unit cell exhibits close structural similarities to those of $Nd_{1.85}Ce_{0.15}CuO_{4-\delta}$. Therefore it is interesting to see whether the electronic parameters are similar to those of the n-doped HTSC's or not.

Figure 13 depicts the Nd $3d_{3/2}$ core-level spectra of Nd_2CuO_4 [13(c)] and $Nd_{1.4}Ce_{0.2}Sr_{0.4}CuO_{4-\delta}$ [13(a) and

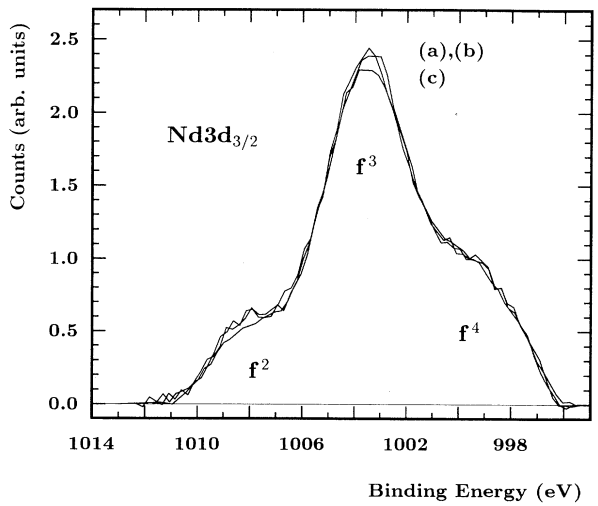

FIG. 13. Nd $3d_{3/2}$ core-level spectra of oxidized (a) and nonoxidized (b) $Nd_{1.4}Ce_{0.2}Sr_{0.4}CuO_{4-\delta}$ aswell as of Nd_2CuO_4 (c). Spectra are normalized onto the $|4f^4\underline{Lc}\rangle$ shoulder.

13(b)]. Both spectra strongly resemble those of trivalent Nd oxide Nd_2O_3:[121] Besides the main peak at $E_B = 1004$ eV there are two satellite lines at higher (1008 eV) and lower (1000 eV) binding energy. Whereas the main feature mostly results from a $4f^3$ final state, the higher- and lower-E_B satellites are due to charge fluctuations with mainly $4f^2$ and $4f^4$ final-state configurations. From the spectra one only can see a little difference of the intensity of the $4f^3$ main peak relative to the $4f^4$ shoulder between Nd_2CuO_4 and $Nd_{1.4}Ce_{0.2}Sr_{0.4}CuO_{4-\delta}$.

Since[79] the usual values for the charge-transfer energy between Nd and O in trivalent Nd oxide compounds are within the order of about 10 eV (Ref. 122) (which is considerably larger than the O $2p$ bandwidth in the rare-earth sheets of about 3 eV obtained form LDA calculations[88]) one may[79] estimate the electronic parameters of the Nd-O sheets by using a simple 2×2 cluster interaction model.[74] For the initial state we take as a basis $|f^3\rangle$ and $|f^3\underline{L}\rangle$ configurations ($\underline{L}$ is the hole in the ligand O $2p$ orbital) with energies 0 and $\tilde{\Delta}$, respectively, and a Nd-O hybridization t. In the final state we have $|f^3\underline{c}\rangle$ and $|f^4\underline{L}\underline{c}\rangle$ states with energies 0 and $\tilde{\Delta}-U_{fc}$, respectively, and hybridization t, too ($\underline{c}$ is the Nd $3d$ core hole). By diagonalizing the Hamiltonian matrices in the initial and final states we can calculate a two-line photoemission spectrum by taking Eq. (2) or (11). Table V shows the values obtained for Nd-O hybridization and the charge-transfer energy calculated from the spectra [taking a Nd $3d$-Nd $4f$ core-hole interaction of U_{fc} of 12.7 eV (Refs. 123 and 122)], which are very similar to the parameters obtained by Ikeda *et al.*[122] for Nd_2O_3 ($\tilde{\Delta}=9.5$ eV; $t=1.59$ eV). Both Nd-O hybridization and the charge-transfer energy are found to be slightly higher for the Nd_2CuO_4 system.

These tendencies are confirmed by the partial Nd $4f$ spectra to be seen in Fig. 14. Partial Nd $4f$ spectra are obtained by recording the valence-band spectra at photon energies $\hbar\omega$ above and below the Nd $4d\rightarrow4f$ resonance threshold at $\hbar\omega=124$ eV. Taking the difference of both energy-dispersion curves (EDC's) one obtains the contributions of Nd $4f$ levels to the valence band. As can be seen in Fig. 14 the partial Nd $4f$ spectra consist of two main features around $E_B=3.5$ eV and $E_B=7$ eV, as is typical for trivalent neodymium oxide.[124] Whereas the lower part of the spectrum can be attributed to localized $4f^2$ final states [final-state multiplet drawn in Fig. 14 (Ref. 125)], the upper part is due to Nd $4f$-O $2p$ hybridized states, corresponding to a $4f^3\underline{L}$ final state. In the case of Nd_2CuO_4, the relative weight of the $|4f^3\underline{L}\rangle$ states is higher and shifted towards lower binding energy, indicating also an enhanced Nd-O hybridization and/or charge-transfer energy for the n-doped compound.

TABLE V. Nd-O charge-transfer energy $\tilde{\Delta}$ and hybridization t for Nd_2CuO_4 and $Nd_{1.4}Ce_{0.2}Sr_{0.4}CuO_{4-\delta}$.

	Nd_2CuO_4	$Nd_{1.4}Ce_{0.2}Sr_{0.4}CuO_{4-\delta}$
$I(f^3)/I(f^4)$	2.84	2.95
$E(f^3)-E(f^4)$ (eV)	4.3	4.3
t (eV)	1.49	1.47
$\tilde{\Delta}$ (eV)	9.65	9.58

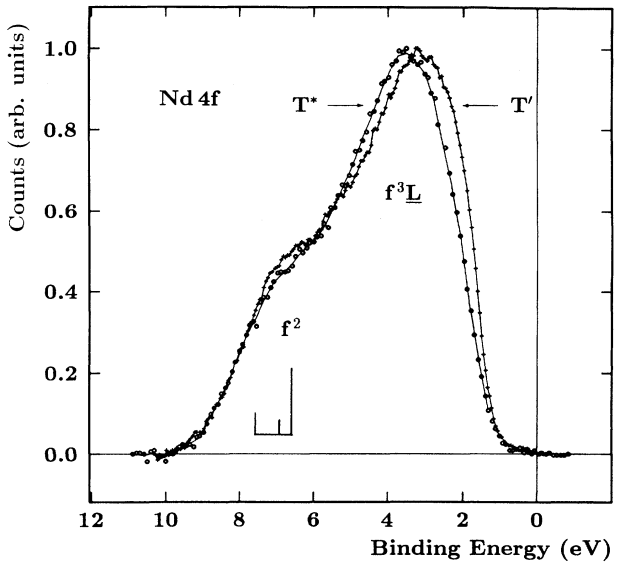

FIG. 14. Partial Nd $4f$ valence-band spectra of $Nd_{1.4}Ce_{0.2}Sr_{0.4}CuO_{4-\delta}$ and Nd_2CuO_4. Also drawn in is the $4f^2$ final-state multiplet (Ref. 126).

As can be seen from Table VI, the mean Nd-O bond lengths in Nd_2CuO_4 and $Nd_{1.4}Ce_{0.2}Sr_{0.4}CuO_{4-\delta}$ differ by about 0.07 Å. The slightly larger Nd-O distance in the T^* compound together with the completely different Nd coordination in the T part of the $Nd_{1.4}Ce_{0.2}Sr_{0.4}CuO_{4-\delta}$ structure (see Fig. 1) should be able to explain the small differences in hybridization and charge-transfer energy obtained from the core-level and valence-band spectra.

For a more detailed analysis of the electronic states of Nd^{3+} in $Nd_{2-x}Ce_xCuO_{4-\delta}$ and $Nd_{1.4}Ce_{0.2}Sr_{0.4}CuO_{4-\delta}$ we consider the magnetic susceptibility $\chi(T)$ of both systems in order to get information on antiferromagnetic correlations and crystal-field splitting of Nd $4f$ levels. For simplicity, we adopt for the T' system (and of course for the T' part of the T^* structure) a cubic instead of the actually slightly tetragonal surrounding of Nd by O. For the T part of the T^* structure we also found the assumption of a cubic surrounding (for which all axes are, in contrast to T', distorted by 45°) to fit the experimental data quite well, despite the actually much more complicated oxygen surrounding of the rare-earth ions in the T structure. We analyze the susceptibility data in terms of the model given by Penney and Schlapp,[126] as was done for $Nd_2CuO_{4-\delta}$ by Saez-Puche *et al.*[28] and Seaman *et al.*[29] and for $Nd_{1.85}Ce_{0.15}CuO_{4-\delta}$ by ourselves.[30]

For the magnetic susceptibility of Nd^{3+} ($J=\frac{9}{2}$) in the presence of a cubic surrounding one has

TABLE VI. Nd-O distance in T' and T^* structures. $\bar{\Sigma}$ denotes the mean Nd-O distance for the whole structure.

	$Nd_{1.85}Ce_{0.15}CuO_{4-\delta}$	$Nd_{1.4}Ce_{0.2}Sr_{0.4}CuO_{4-\delta}$	
		T part	T' part
	2.50 Å	2.69 Å	2.44 Å
$\bar{\Sigma}$	2.50 Å	2.57 Å	
Reference	92	7	

$$\chi_{Nd^{3+}}=\frac{2ng^2\mu_B^2\mu_0}{A}[0.1483e^{19.59\beta A}+0.2396e^{-9.11\beta A}-0.3879e^{-20.95\beta A}$$
$$+\beta A(6.065e^{19.59\beta A}+4.031e^{-9.11\beta A}+1.680e^{-20.95\beta A})]/(2e^{19.59\beta A}+2e^{-9.11\beta A}+e^{-20.95\beta A}),$$

where A is the total multiplet width of the crystal-field-split Nd $4f$ levels divided by 40.54 and g the Landé factor. Provided $M(H)$ is approximately proportional to H, antiferromagnetic correlations between Nd ions can be taken into account by adding a mean-field term to Eq. (13):

$$\frac{1}{\chi}=\frac{1}{\chi_{Nd^{3+}}}+\frac{\Theta_{Nd}}{C_{Nd}}, \tag{14}$$

with C_{Nd} being the ordinary Curie constant of the Nd system. Contributions of Cu^{2+} can be neglected since due to strong antiferromagnetic correlations the magnetic moment of the paramagnetic Cu spins is very small for HTSC cuprates [$Nd_{1.85}Ce_{0.15}CuO_{4-\delta}$, $\approx 0.45\mu_B$ (Refs. 127 and 128)].

Figure 15 shows the measured and calculated inverse magnetic susceptibilities for $Nd_{1.85}Ce_{0.15}CuO_{4-\delta}$ and $Nd_{1.4}Ce_{0.2}Sr_{0.4}CuO_{4-\delta}$. For the T^* compounds our experimental results are in good agreement with those of Ikegawa *et al.*[129] The parameters of the fit after Eq. (14) are given in Table VII.

The value for the total CF splitting for

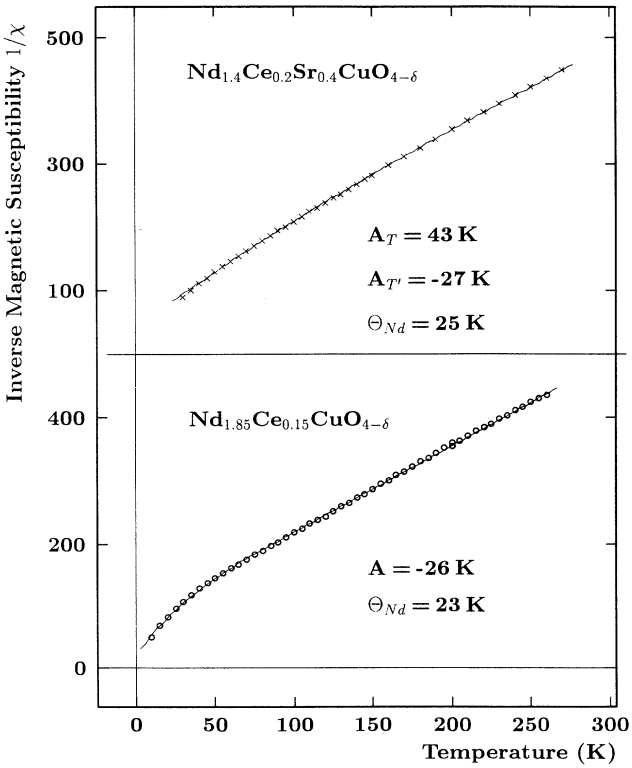

FIG. 15. Magnetic susceptibility $\chi(T)$ of $Nd_{1.4}Ce_{0.2}Sr_{0.4}CuO_{4-\delta}$ (upper part) and $Nd_{1.85}Ce_{0.15}CuO_{4-\delta}$ (lower part). Solid lines are the best fit to the data after the model described in the text [Eq. (14)].

$Nd_{1.85}Ce_{0.15}CuO_{4-\delta}$ of 91 meV is in very good agreement with the multiplet width of 93 meV reported from neutron-scattering experiments.[130–132] The larger crystal-field splitting of Nd $4f$ in the T' part of the $Nd_{1.4}Ce_{0.2}Sr_{0.4}CuO_{4-\delta}$ structure compared to $Nd_{1.85}Ce_{0.15}CuO_{4-\delta}$ could be explained by the smaller Nd-O distance in this structural element as can be seen from Table VI. The comparatively high value of the antiferromagnetic Curie temperature observed for the T^* compounds seems remarkable. Further experiments will show whether there is antiferromagnetic order of Nd moments in $Nd_{1.4}Ce_{0.2}Sr_{0.4}CuO_{4-\delta}$, too.

Since in the description of the magnetic-susceptibility measurements it was not necessary to take into account any contributions of doped Ce ions neither for $Nd_{1.85}Ce_{0.15}CuO_{4-\delta}$ nor for $Nd_{1.4}Ce_{0.2}Sr_{0.4}CuO_{4-\delta}$, one should presume the Ce dopants in both compounds to be tetravalent. This is confirmed by the XPS Ce $3d$ core-level spectra as shown in Fig. 16. We compare the measurements on $Nd_{1.85}Ce_{0.15}CuO_{4-\delta}$, oxidized and nonoxidized $Nd_{1.4}Ce_{0.2}Sr_{0.4}CuO_{4-\delta}$. There are no significant differences between the three curves. All of them strongly resemble the Ce $3d$ spectrum of tetravalent CeO_2,[133] as was already found by Grassmann *et al.*[25] for $Nd_{1.85}Ce_{0.15}CuO_{4-\delta}$ and by Izumi *et al.*,[7] Tokura *et al.*,[22] and ourselves[49] for $Nd_{1.4}Ce_{0.2}Sr_{0.4}CuO_{4-\delta}$. From the intensity ratios and energy positions of the three features in the Ce $3d$ spectra (labeled in the figure by the final-state designations $4f^0$, $4f^1$, and $4f^2$) we find by a single-impurity Anderson calculation a mean $4f$ occupancy in the initial state of $n_f \approx 0.4$. This is very similar to the value of $n_f \approx 0.5$ found for CeO_2 by Wouilloud *et al.*[34] Despite this n-type doping by Ce^{4+} in $Nd_{1.4}Ce_{0.2}Sr_{0.4}CuO_{4-\delta}$, negative-charge carriers apparently fail to become intrinsic in the Cu-O layers as in the case of $Nd_{1.85}Ce_{0.15}CuO_{4-\delta}$ and/or are overwhelmed by hole doping with divalent Sr.

2. $Sr_{0.85}Nd_{0.15}CuO_{2-\delta}$ systems

Already Smith *et al.*[5] presumed the Nd dopants in $Sr_{0.85}Nd_{0.15}CuO_{2-\delta}$ to be trivalent from the Nd-doping dependence of the lattice parameters. Valence-band photoemission may help to clear up this point by recording

TABLE VII. Fit parameters for the magnetic susceptibility of $Nd_{1.85}Ce_{0.15}CuO_{4-\delta}$ and $Nd_{1.4}Ce_{0.2}Sr_{0.4}CuO_{4-\delta}$.

	$Nd_{1.85}Ce_{0.15}CuO_{4-\delta}$	$Nd_{1.4}Ce_{0.2}Sr_{0.4}CuO_{4-\delta}$	
		T part	T' part
A[a] (K)	−26	43	−27
Θ_{Nd}[b] (K)	−20	−25	

[a]Total crystal-field splitting, divided by 40.54.
[b]Antiferromagnetic Curie temperature.

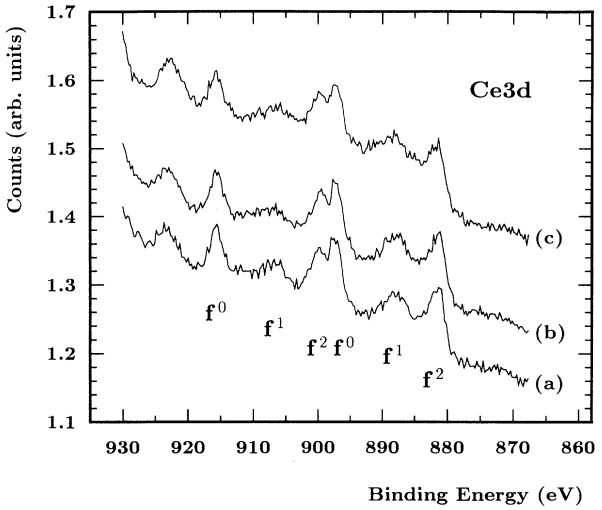

FIG. 16. Ce $3d_{3/2}$ core-level spectra of oxidized (a) and nonoxidized (b) $Nd_{1.4}Ce_{0.2}Sr_{0.4}CuO_{4-\delta}$ as well as of Nd_2CuO_4 (c).

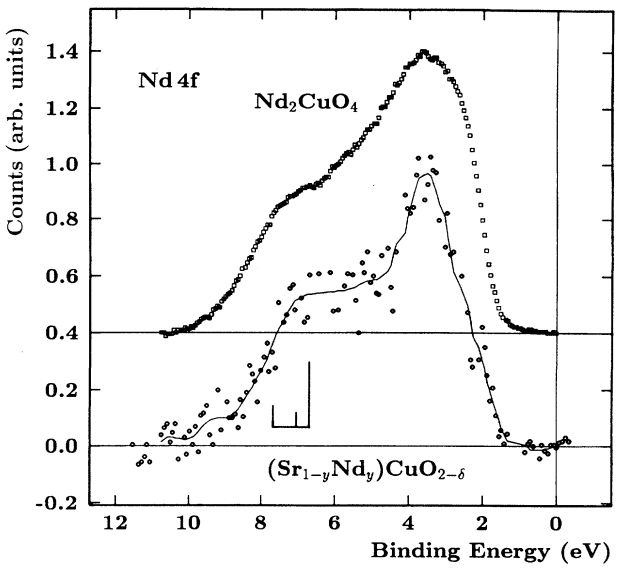

FIG. 17. Partial Nd $4f$ valence-band spectra of Nd_2CuO_4 (upper part) and $Sr_{0.85}Nd_{0.15}CuO_{2-\delta}$ (lower part). Also drawn in is the $4f^2$ final-state multiplet (Ref. 125).

the partial Nd $4f$ spectrum of the doped ions. Figure 17 depicts the partial Nd valence bands of $Nd_2CuO_{4-\delta}$ and $Sr_{0.85}Nd_{0.15}CuO_{2-\delta}$. Because of the very small $Sr_{0.85}Nd_{0.15}CuO_{2-\delta}$ samples and since Nd is only the dopant element in this system, the signal-to-noise ratio is not very good for the infinite-layer compound. Nevertheless, the general shape of trivalent Nd-O compounds with localized $|4f^2\rangle$ and O $2p$ hybridized $|4f^3\underline{L}\rangle$ final states can be recognized very well from the data, which confirms the $Sr_{0.85}Nd_{0.15}CuO_{2-\delta}$ system to be a further electron-doped high-T_c cuprate.

IV. SUMMARY

The electronic structure of several p- and n-doped high-T_c superconductors or their parent compounds, respectively, has been investigated by means of photoelectron spectroscopy and auxiliary measurements. Compounds under consideration were the p-doped $Nd_{1.4}Ce_{0.2}Sr_{0.4}CuO_{4-\delta}$ of the T^* structure as well as the n-doped systems $Nd_{2-x}Ce_xCuO_{4-\delta}$ and $Sr_{0.85}Nd_{0.15}CuO_{2-\delta}$.

Evaluation of core-level and valence-band spectra by means of an Anderson impurity and a CuO_4 (CuO_5) cluster model, respectively, gives—compared to T^* compounds—a quite high value of the Cu $3d$ Coulomb correlation energy for both n-type HTSC's, $Nd_{1.85}Ce_{0.15}CuO_{4-\delta}$, and $Sr_{0.85}Nd_{0.15}CuO_{2-\delta}$. We attribute these findings to a lower delocalization probability for two holes at the copper site in the case of electron-doped high-T_c cuprates. We presume this high correlation energy to prevent doped electrons to become localized at the copper site, thus being a kind of criterion for n-type high-T_c superconductivity. For the $Sr_{0.85}Nd_{0.15}CuO_{2-\delta}$ system we find a remarkably low Cu-O hybridization which could, besides the lacking apical oxygen, account for the high value of U_{dd}.

Investigations of Nd-O sheets in $Nd_{2-x}Ce_xCuO_{4-\delta}$ and $Nd_{1.4}Ce_{0.2}Sr_{0.4}CuO_{4-\delta}$ show quite similar characteristics in the electronic properties (besides small differences in Nd-O hybridization and the charge-transfer energy). Evaluation of the normal-state magnetic susceptibilities thus gives very similar antiferromagnetic correlations between Nd spins in both systems.

The valence states of cerium in $Nd_{1.85}Ce_{0.15}CuO_{4-\delta}$ and $Nd_{1.4}Ce_{0.2}Sr_{0.4}CuO_{4-\delta}$ and of Nd dopants in $Sr_{0.85}Nd_{0.15}CuO_{2-\delta}$ have been investigated by core-level and resonant valence-band photoemission. Whereas Ce is confirmed to be tetravalent in the T' and T^* systems, we find Nd to be trivalent in $Sr_{0.85}Nd_{0.15}CuO_{2-\delta}$. This corroborates again that the infinite-layer compound is a further n-doped high-T_c cuprate.

ACKNOWLEDGMENTS

It is a pleasure for us to gratefully acknowledge Professor G. A. Sawtazky for his hospitality for one of us (M.K.) and for helpful discussions. To Dr. H. Eskes we are gratefully indebted due to his great advisory support for performing many of the calculations. Also we would like to thank Professor L. Ley for helpful discussions. Professor H. Burzlaff and G. Brüderl are gratefully acknowledged for performing the structure refinements on the infinite layer compound. This work was supported by the Bundesministerium für Forschung und Technologie and the "Bayerische Forschungsstiftung Hochtemperatursupraleitung" (FORSUPRA).

*Also at Institut für Anorganische Chemie, Universität Regensburg, Universitätstrasse 1, D-W 8400 Regensburg, Germany.

†Also at Institut für Experimentalphysik, Universität Hamburg, Luruper Chaussee 122, D-W 2000 Hamburg, Germany.

[1]Y. Tokura, H. Takagi, and S. Uchida, Nature **337**, 345 (1989).

[2]H. Takagi, S. Uchida, and Y. Tokura, Phys. Rev. Lett. **62**, 1197 (1989).

[3]J. T. Markert, E. A. Early, T. Bjørnholm, S. Ghamaty, B. W. Lee, J. J. Neumeier, R. D. Price, C. L. Seaman, and M. B. Maple, Physica C **158**, 178 (1989).

[4]J. Akimitsu, S. Suzuki, M. Watanabe, and H. Sawa, Jpn. J. Appl. Phys. **27**, L1859 (1988).

[5]M. G. Smith, A. Manthiram, J. Zhou, J. B. Goodenough, and J. T. Markert, Nature **351**, 549 (1991).

[6]H. Sawa, S. Suzuki, M. Watanabe, J. Akimitsu, H. Matsubara, H. Watabe, S. Uchida, K. Kokusho, H. Asano, F. Izumi, and E. Takayama-Muromachi, Nature **337**, 347 (1989).

[7]F. Izumi, E. Takayama-Muromachi, A. Fujimori, T. Kamiyama, H. Asano, J. Akimitsu, and H. Sawa, Physica C **158**, 440 (1989).

[8]H.-K. Müller-Buschbaum and W. Wollschläger, Z. Anorg. Chem. **414**, 76 (1975).

[9]H.-K. Müller-Buschbaum, Angew. Chem. **89**, 89 (1977).

[10]C. Michel and B. Raveau, Rev. Chim. Miner. **21**, 407 (1984).

[11]Y. Tokura, H. Takagi, H. Watanabe, H. Matsubara, S. Uchida, K. Hiraga, T. Mochiku, and H. Asano, Phys. Rev. B **40**, 2568 (1989).

[12]E. Takayama-Muromachi, S. Uchida, M. Kobayashi, and K. Kato, Physica C **166**, 449 (1989).

[13]S. W. Cheong, Z. Fisk, J. D. Thompson, and R. B. Schwartz, Physica C **159**, 407 (1989).

[14]N. Ohashi, H. Ikawa, O. Fukunaga, and J. Tanaka, Physica C **166**, 465 (1990).

[15]N. Ohashi, H. Ikawa, O. Fukunaga, M. Kobayashi, and J. Tanaka, Physica C **177**, 377 (1991).

[16]K. Takahashi, B. Okai, M. Kosuge, and M. Ohta, Jpn. J. Appl. Phys. **27**, L1374 (1988).

[17]M. J. Rosseinsky, K. Prassides, and P. Day, Physica C **161**, 21 (1989).

[18]T. Sakurai, T. Yamashita, H. Yamauchi, and S. Tanaka, Physica C **161**, 6 (1989).

[19]M. Kosuge, S. Ikegawa, N. Koshizuka, and S. Tanaka, Physica C **176**, 373 (1991).

[20]S. Ikegawa, T. Wada, T. Yamashita, H. Yamauchi, and S. Tanaka, Phys. Rev. B **45**, 5659 (1992).

[21]N. A. Fortune, K. Murata, Y. Yokoyama, M. Ishibashi, and Y. Nishinara, Physica C **178**, 437 (1991); T. Terashima, Y. Bando, K. Iijima, K. Yamamoto, K. Hirata, K. Hayashi, Y. Matsuda, and S. Komiyama, Appl. Phys. Lett. **56**, 677 (1990).

[22]Y. Tokura, A. Fujimori, H. Matsubara, H. Watabe, H. Takagi, S. Uchida, M. Sakai, H. Ikeda, S. Okuda, and S. Tanaka, Phys. Rev. B **39**, 9704 (1989).

[23]J. M. Tranquada, S. M. Heald, A. R. Moodebaugh, C. Liang, and M. Croft, Nature **337**, 720 (1989).

[24]E. E. Alp, S. M. Mini, M. Ramanathan, B. Dabrowski, D. R. Richards, and D. G. Hinks, Phys. Rev. B **40**, 2617 (1989).

[25]A. Grassmann, J. P. Ströbel, M. Klauda, J. Schlötterer, and G. Saemann-Ischenko, Europhys. Lett. **9**, 827 (1989).

[26]M. Klauda, J. P. Ströbel, J. Schlötterer, A. Grassmann, J. Markl, and G. Saemann-Ischenko, Physica C **173**, 109 (1991).

[27]M. Alexander, H. Romberg, N. Nücker, P. Adelmann, J. Fink, J. T. Markert, M. B. Maple, S. Uchida, H. Takagi, Y. Tokura, A. C. P. W. James, and D. W. Murphy, Phys. Rev. B **43**, 333 (1991).

[28]R. Saez-Puche, M. Norton, T. R. White, and W. S. Glaunsinger, J. Solid State Chem. **50**, 281 (1983).

[29]C. L. Seaman, N. Y. Ayoub, T. Bjørnholm, E. A. Early, S. Ghamaty, B. W. Lee, J. T. Markert, J. J. Neumeier, P. K. Tsai, and M. B. Maple, Physica C **159**, 391 (1989).

[30]M. Klauda, J. P. Ströbel, M. Lippert, G. Saemann-Isschenko, W. Gerhäuser, and H.-W. Neumüller, Physica C **165**, 251 (1990).

[31]J. W. Lynn, I. W. Sumarlin, S. Skanthakumar, W.-H. Li, R. N. Shelton, J. L. Peng, Z. Fisk, and S.-W. Cheong, Phys. Rev. B **41**, 2569 (1990).

[32]J. P. Ströbel, M. Klauda, H. Weinfurther, J. Markl, M. Steiner, G. Saemann-Ischenko, and K.-F. Renk, Physica B **169**, 695 (1991).

[33]B. Jiang, B.-H. Oh, and J. T. Markert, Phys. Rev. B **45**, 2311 (1992).

[34]T. Siegrist, S. M. Zahurak, D. W. Murphy, and R. S. Roth, Nature **334**, 231 (1988).

[35]C. L. Teske and H.-K. Müller-Buschbaum, Z. Anorg. Allg. Chem. **379**, 234 (1970).

[36]M. Takano, Y. Takeda, H. Okada, M. Miyamoto, and T. Kusaka, Physica C **159**, 375 (1989).

[37]M. Takano, M. Azuma, Z. Hiroi, Y. Bando, and Y. Taekada, Physica C **176**, 441 (1991).

[38]G. Er, Y. Miyamoto, F. Kanamaru, and S. Kirkkigawa, Physica C **181**, 206 (1991).

[39]W. Korczak, M. Perroux, and P. Strobel, Physica C **193**, 303 (1992).

[40]R. J. Cava, Nature **351**, 518 (1991).

[41]J. B. Goodenough, Supercond. Sci. Technol. **3**, 26 (1990).

[42]J. B. Goodenough and A. Manthiram, J. Solid State Chem. **88**, 115 (1990).

[43]G. Er, S. Kikkawa, F. Kanamaru, Y. Miyamoto, S. Tanaka, M. Sera, M. Sato, Z. Hiroi, M. Takano, and Y. Bando, Physica C **196**, 271 (1992).

[44]S. Uchida, H. Takagi, Y. Tokura, N. Koshihara, and T. Arima, in *Strong Correlation and Superconductivity,* edited by H. Fukuyama and S. Maekawa (Springer, Berlin, 1989), p. 194.

[45]H. Adachi, T. Satoh, Y. Ichikawa, K. Setsune, and K. Wasa, Physica C **196**, 14 (1992).

[46]N. Sugii, M. Ichikawa, K. Kubo, T. Sakurai, K. Yamamoto, and H. Yamauchi, Physica C **196**, 129 (1992).

[47]For an overview, see, e.g., J. Fink, J. Pflüger, Th. Müller-Heinzerling, N. Nücker, B. Scheerer, H. Romberg, M. Alexander, R. Manzke, T. Buslaps, R. Claessen, and M. Skibowski, in *Earlier and Recent Aspects of Superconductivity,* edited by K. A. Müller and G. Bednorz, Springer Series in Solid State Science Vol. 90 (Springer, Berlin, 1990); K. Kitazawa, in *Earlier and Recent Aspects of Superconductivity,* edited by K. A. Müller and G. Bednorz, Springer Series in Solid State Science Vol. 90 (Springer, Berlin, 1990); F. Al Shamma and J. C. Fuggle, Physica C **169**, 325 (1990), and references therein.

[48]N. Ohashi, H. Ikawa, and O. Fukunaga, Physica C **190**, 154 (1991).

[49]M. Klauda, P. Lunz, J. Markl, J. P. Ströbel, C. Fink, and G. Saemann-Ischenko, Physica C **191**, 137 (1992).

[50]M. Klauda, P. Lunz, J. Markl, C. Fink, G. Saemann-Ischenko, R. Seemann, and R. L. Johnson, in Electronic Properties of High-T_c Superconductors, Springer Series in Solid State Science Vol. 113 (Springer, Berlin, 1993).

[51]M. Kosuge and K. Kurusu, Jpn. J. Appl. Phys. **28**, L810 (1989).

[52]M. Kosuge, Jpn. J. Appl. Phys. **28**, L49 (1989).
[53]M. Sato, M. Sera, S. Shamamoto, M. Onoda, S. Yamagata, and H. Fujishita (unpublished).
[54]J. P. Ströbel, A. Thomä, B. Hensel, H. Adrian, and G. Saemann-Ischenko, Physica C **153-155**, 1537 (1988).
[55]See, e.g., M. Kosuge, S. Ikegawa, N. Koshizuka, and S. Tanaka, Physica C **176**, 373 (1991).
[56]J. P. Ströbel, M. Klauda, J. Markl, and G. Saemann-Ischenko, Jpn. J. Appl. Phys. **29**, 1439 (1990).
[57]T. Robert, M. Bartel, and G. Offergeld, Surf. Sci. **33**, 123 (1972).
[58]W. Schindler, A. Grassmann, P. Schmitt, J. P. Ströbel, H. Niederhofer, G. Adrian, G. Saemann-Ischenko, and H. Adrian, Jpn. J. Appl. Phys. **26**, 1199 (1987).
[59]A. Grassmann, Ph.D. thesis, Universität Erlangen, Germany, 1990.
[60]G. Rietveld, M. Glastra, S. M. Verbrugh, O. Jepsen, O. K. Anderson, and D. van der Marel, Physica C **185-189**, 829 (1991).
[61]P. Adler and A. Simon, Z. Phys. B **85**, 197 (1991).
[62]P. A. P. Lindberg, Z.-X. Shen, W. E. Spicer, and I. Lindau, Surf. Sci. Rep. **11**, 1 (1990).
[63]A. J. Arko, R. S. List, R. J. Bartlett, S.-W. Cheong, Z. Fisk, J. D. Thompson, C. G. Olson, A.-B. Yang, R. Liu, C. Gu, B. W. Veal, J. Z. Liu, A. P. Paulikas, K. Vandervoort, H. Claus, J. C. Compuzano, and J. E. Schirber, Phys. Rev. B **40**, 2268 (1989).
[64]H. Buchkremer-Hermanns, P. Adler, and A. Simon, J. Less Common Met. **164/165**, 760 (1990).
[65]Y. Fukuda, T. Suzuki, M. Nagoshi, Y. Syono, K. Oh-Ishi, and M. Tachiki, Solid State Commun. **72**, 1183 (1989).
[66]Y. H. Sakisaka, T. Maruyama, Y. Morikawa, H. Kato, K. Edamoto, M. Okusawa, Y. Aiura, H. Yanashima, T. Terashima, Y. Bando, K. Bando, K. Iijima, K. Yamamoto, and K. Hirata, Solid State Commun. **74**, 609 (1990).
[67]J. W. Allen, C. G. Olson, M. B. Maple, J.-S. Kang, L. Z. Liu, J.-H. Park, R. O. Anderson, W. P. Ellis, J. T. Markert, Y. Dalichaouch, and R. Liu, Phys. Rev. Lett. **64**, 595 (1990).
[68]S. Mazumdar, Physica C **161**, 423 (1989).
[69]J. B. Torrance and R. M. Metzger, Phys. Rev. Lett. **63**, 1515 (1989).
[70]R. P. Gupta and M. Gupta, Physica C **160**, 129 (1989); **162-164**, 1437 (1989).
[71]S. Uji, M. Shimoda, and H. Aoki, Jpn. J. Appl. Phys. **28**, L804 (1989).
[72]Y. Hwu, M. Marsi, A. Terrasi, R. Rioux, Y. Chang, J. T. McKinley, M. Onellion, G. Margaritondo, M. Capozi, C. Quaresima, A. Campo, C. Ottaviani, P. Perfetti, N. G. Stoffel, and E. Wang, Phys. Rev. B **43**, 2678 (1991).
[73]S. Larsson, Chem. Phys. Lett. **32**, 401 (1975).
[74]G. van der Laan, C. Westra, C. Haas, and G. Sawatzky, Phys. Rev. B **23**, 4369 (1981).
[75]G. A. Sawatzky, in *Studies in Inorganic Chemistry,* edited by R. Metselaar, H. J. M. Heijligers, and J. Schoonman (Elsevier, Amsterdam, 1983), Vol. 3, p. 3.
[76]O. Gunnarson and K. Schönhammer, Phys. Rev. B **28**, 4315 (1983).
[77]O. Gunnarson and K. Schönhammer, Phys. Rev. B **31**, 4815 (1985).
[78]A. Fujimori and F. Minami, Phys. Rev. B **28**, 4489 (1983).
[79]J. Zaanen, C. Westra, and G. A. Sawatzky, Phys. Rev. B **33**, 8060 (1986).
[80]P. W. Anderson, Phys. Rev. **124**, 41 (1961).
[81]K. Okada and A. Kotani, J. Electron Spectrosc. Relat. Phenom. **52**, 313 (1990); J. Phys. Soc. Jpn. **58**, 2578 (1989).
[82]A. E. Bocquet, T. Mizokawa,T. Saitoh, H. Namatame, and A. Fujimori, Phys. Rev. B **46**, 3771 (1992).
[83]J. M. Tranquada, S. M. Heald, W. Kunnmann, A. R. Moodenbaugh, S. L. Qiu, Y. Xu, and P. K. Davies, Phys. Rev. B **44**, 5176 (1991).
[84]K Okada and A. Kotani, J. Phys. Soc. Jpn. **58**, 1095 (1989).
[85]See, e.g., for $La_{2-x}Sr_xCuO_{4-\delta}$, P. Steiner, J. Albers, V. Kinsinger, I. Sander, B. Siegwart, S. Hüfner, and C. Politis, Z. Phys. B **66**, 275 (1987).
[86]S. Massida, N. Hamada, J. Yu, and A. J. Freeman, Physica C **157**, 571 (1989).
[87]K. Takegahara and T. Kasuya, Solid State Commun. **70**, 637 (1989).
[88]Z. Szotek, G. Y. Guo, and W. M. Temmerman, Physica C **175**, 1 (1991).
[89]S. P. Kowalczyk, L. Ley, F. R. McFeely, and D. A. Shirley, Phys. Rev. B **11**, 1721 (1975).
[90]J. Zaanen and G. A. Sawatzky, Phys. Rev. B **33**, 8074 (1986).
[91]A. Fujimori, E. Takayama-Muromachi, Y. Uchida, and B. Okai, Phys. Rev. B **35**, 8814 (1987).
[92]E. F. Paulus, I. Yehia, H. Fuess, J. Rodriguez, T. Vogt, J. P. Ströbel, M. Klauda, and G. Saemann-Ischenko, Solid State Commun. **73**, 791 (1990).
[93]P. V. P. S. S. Sastry, I. K. Gopalakrishnan, A. Sequiera, H. Rajagopal, K. Gangadharan, G. M. Phatak, and R. M. Iyer, Physica C **156**, 230 (1988).
[94]W. A. Harrison, *Electronic Structure and the Properties of Solids* (Freeman, San Francisco, 1980).
[95]E. Antonides, E. C. Janse, and G. A. Sawatzky, Phys. Rev. B **15**, 1669 (1977).
[96]The two-hole density of states for two noncorrelated valence-band holes simply is given by the convolution of two one-particle DOS for one hole.
[97]M. Cini, Solid State Commun. **24**, 681 (1977).
[98]H. W. Haak, G. A. Sawatzky, and T. D. Thomas, Phys. Rev. Lett. **41**, 1825 (1978).
[99]R. Hoogewijs, L. Fiermans, and J. Vennik, Chem. Phys. Lett. **38**, 471 (1976).
[100]F. U. Hillebrecht, J. Fraxedas, L. Ley, H. J. Trodahl, and J. Zaanen, Phys. Rev. B **38**, 12 442 (1988).
[101]See, e.g., J. C. Fuggle, P. J. W. Weijs, R. Schoorl, G. A. Sawatzky, J. Fink, N. Nücker, P. J. Durham, and W. M. Temmerman, Phys. Rev. B **37**, 123 (1988).
[102]Atomic subshell photoionization cross sections for O $2p$ and Cu $3d$, $\sigma_{O\,2p}/\sigma_{Cu\,3d}$ ($\hbar\omega=20$ eV)$=1.43$, $\sigma_{O\,2p}/\sigma_{Cu\,3d}$ ($\hbar\omega=40$ eV)$=0.69$, from J. J. Yeh and I. Lindau, At. Data Nucl. Data Tables **32**, 1 (1985).
[103]W. E. Pickett, Rev. Mod. Phys. **61**, 433 (1989).
[104]M. R. Thuler, R. L. Benbow, and Z. Hurych, Phys. Rev. B **26**, 669 (1982).
[105]H. Eskes, L. H. Tjeng, and G. A. Sawatzky, Phys. Rev. B **41**, 288 (1990).
[106]G. A. Sawatzky, in *Core Level Spectroscopy in Condensed Systems,* edited by J. Kanamori and A. Kotani, Springer Series in Solid State Science Vol. 81 (Springer, Berlin, 1988), p. 99.
[107]A. Fujimori, Phys. Rev. B **39**, 793 (1989).
[108]J. C. Slater, *Quantum Theory of Atomic Structure* (McGraw-Hill, New York, 1960).
[109]J. S. Griffith, *The Theory of Transition Metal Ions* (Cambridge University Press, Cambridge, 1961).
[110]C. E. Moore, *Atomic Energy Levels,* Natl. Bur. Stand. (U.S.) Circ. No. 467 (U.S. GPO, Washington, DC, 1958).
[111]H. Eskes, G. A. Sawatzky, and L. F. Feiner, Physica C **160**,

424 (1989).
[112]H. Eskes and G. A. Sawatzky, Phys. Rev. Lett. **61**, 1415 (1988).
[113]T. Tohyama, Y. Ohta, and S. Maekawa, Physica C **158**, 525 (1989).
[114]Because of different screening processes in the final states of Cu $2p$ and Cu $3d$ photoemission, one may not suppose to obtain equal values for the charge-transfer energy $\tilde{\Delta}$ and Δ, respectively, from these two different spectroscopies. The same arguments of course also hold for the values for U_{dd}^{eff} and $U_{dd}(^1G)=A+4B+2C$, obtained from Auger spectroscopy and valence-band investigations, respectively.
[115]Z. X. Shen, J. W. Allen, J. J. Yeh, J.-S. Kang, W. Ellis, W. Spicer, I. Lindau, M. B. Maple, Y. D. Dalichaouch, M. S. Torikachvili, J. Z. Sun, and T. H. Geballe, Phys. Rev. B **36**, 8414 (1987).
[116]C. L. Wooten, Beom-haon O, J. T. Markert, M. G. Smith, A. Manthiram, J. Zhou, and J. B. Goodenough, Physica C **192**, 13 (1992).
[117]C. Murayama, N. Môri, S. Yomo, H. Takagi, S. Uchida, and Y. Tokura, Nature **339**, 293 (1989); J. T. Markert, J. Beille, J. J. Neumeier, E. A. Early, C. L. Seaman, T. Moran, and M. B. Maple, Phys Rev. Lett. **64**, 80 (1990).
[118]H. Matsuo, Y. Koike, T. Noji, N. Kobayashi, and Y. Saito, Physica C **196**, 276 (1992).
[119]A. Grassmann, M. Klauda, G. Saemann-Ischenko, and R. L. Johnson, Physica B **161**, 261 (1989).
[120]See, e.g., S. Uchida, H. Takagi, and Y. Tokura, Physica C **162-164**, 1677 (1989).
[121]J. C. Fuggle, M. Campagna, Z. Zolnierek, R. Lässler, and A. Platru, Phys. Rev. Lett. **45**, 1597 (1980).
[122]T. Ikeda, K. Okada, H. Ogasawara, and A. Kotani, J. Phys. Soc. Jpn. **59**, 622 (1990).
[123]As discussed already for the Cu $2p$ spectra, the choice of a constant U_{fc} is somewhat arbitrary, since U_{fc} depends via $U_{fc}\sim U_{ff}$ also on the structural characteristics of the compound under consideration.
[124]J. Schmidt-May, Ph.D. thesis, Universität Hamburg, Germany, 1985.
[125]L. Ley and M. Cardona, *Photoemission in Solids II* (Springer, Berlin, 1979), p. 222.
[126]W. G. Penney and R. Schlapp, Phys. Rev. **41**, 194 (1932).
[127]P. Allenspach, S.-W. Cheong, A. Dommann, P. Fischer, Z. Fisk, A. Furrer, H. R. Ott, and B. Rupp, Z. Phys. B **77**, 185 (1989).
[128]T. Chattopadhyay, P. J. Brown, and U. Köbler, Physica C **177**, 294 (1991).
[129]S. Ikegawa, T. Yamashita, T. Sakurai, R. Itti, H. Yamauchi, and S. Tanaka, Phys. Rev. B **43**, 2885 (1991).
[130]A. T. Boothroyd, S. M. Doyle, D. McK. Paul, and D. S. Misra, Physica C **165**, 17 (1990); A. T. Boothroyd, S. M. Doyle, D. McK. Paul, and R. Osborn, Phys. Rev. B **45**, 10075 (1992).
[131]Y. U. Muzichka, E. A. Goremychkin, I. V. Sashin, M. Diviš, V. Nekvasil, M. Nevřiva, and G. Fillion, Solid State Commun. **82**, 461 (1992).
[132]U. Staub, P. Allenspach, A. Furrer, H. R. Ott, S.-W. Cheong, and Z. Fisk, Solid State Commun. **75**, 431 (1992).
[133]A. Fujimori, Phys. Rev. B **28**, 2281 (1983).
[134]E. Wouilloud, B. Delley, W.-D. Schneider, and Y. Baer, J. Magn. Magn. Mater. **47&48**, 197 (1985).